Scientific Research Publishing

Advances in Nanoparticles, 2022, 11, 73-109
https://www.scirp.org/journal/anp
ISSN Online: 2169-0529
ISSN Print: 2169-0510

In Vivo Animal Model Evaluation of a Powerful Oral Nanomedicine for Treating Breast Cancer in BALB/c Mice Using 4T1 Cell Lines without Chemotherapy

Zahra Fakhroueian[1*], Alireza Massiha[2], Pegah Esmaeilzadeh[3], Mehdi Assmar[4], Afshin Zahedi[5], Pouriya Esmaeilzadeh[6*], Sara Rezaei[7], Shahab Rabiei Lalehdasht[8]

[1]School of Chemical Engineering (Nanomedicine), College of Engineering, University of Tehran, Tehran, Iran
[2]Department of Biotechnology, Lahijan Branch, Islamic Azad University, Lahijan, Iran
[3]Institute of Pharmacy, Martin Luther University Halle Wittenberg, Halle (Saale), Germany
[4]Department of Microbiology, Lahijan Branch, Islamic Azad University, Lahijan, Iran
[5]Department of Veterinary Pathology, Islamic Azad University, Rasht Branch, Rasht, Iran
[6]Department of Chemical Engineering, Sharif University of Technology, Tehran, Iran
[7]Research Department, Production and Laboratory Company ZFP, Rasht, Iran
[8]Department of Biology, Faculty of Science, Rasht Branch Islamic Azad University, Guilan, Iran
Email: *fakhroueian@ut.ac.ir, *pouriya.esmaeilzadeh@gmail.com

How to cite this paper: Fakhroueian, Z., Massiha, A., Esmaeilzadeh, P., Assmar, M., Zahedi, A., Esmaeilzadeh, P., Rezaei, S. and Lalehdasht, S.R. (2022) *In Vivo* Animal Model Evaluation of a Powerful Oral Nanomedicine for Treating Breast Cancer in BALB/c Mice Using 4T1 Cell Lines without Chemotherapy. *Advances in Nanoparticles*, **11**, 73-109.
https://doi.org/10.4236/anp.2022.113006

Received: June 24, 2022
Accepted: August 28, 2022
Published: August 31, 2022

Abstract

Nanopharmaceuticals containing quantum dot nanoparticles (Q-Dot NPs) for treating serious cancers such as breast cancer have made fantastic proposals. In this study, ZnO quantum dot NPs are formulated via ZnO@PVP nanopolymer as co-assistants coordinating with efficacious suitable wetting agents, PEG-binding compound, and W/O emulsifier for producing eco-friendly water-based nanodrug. Several characterization techniques containing SEM, TEM, FTIR, photoluminescence, zeta potential, and UV-Vis absorption were employed for ZnO Q-Dot NPs in nanodrug. This work aims to investigate the anti-tumor effects of such nanomedicine on the 4T1 breast cancer cell line in BALB/c mice, being elaborated through intraperitoneal, injection (IVP) and oral therapy. The impressive findings showed that ZnO nanodrug caused changes in blood factors, having the most effectiveness at 40 μg/ml concentration after two weeks of oral treatments. The significant increase in white blood cells (WBC) neutrophils and meaningful decreases in lymphocytes and especially cholesterol were powerful simultaneous impacts, successfully treating malignant breast cancer masses. In this significant animal model research for breast cancer, the sick mice recovered entirely and even had a safe space to mate. Histopathological results showed no evidence of breast tumor

formation or metastasis in the group treated with nanodrug and their children. This nanomedicine has a therapeutic effect, and is ready to be applied for treating volunteer breast cancer patients. However, its prevention (inhibitory) effect can also be analyzed and added to current data in future studies.

Keywords

Nanomedicine, Nanodrug, ZnO Q-Dot NPs, *In Vivo* Breast Cancer, BALB/c Mice, 4T1 Cell Lines, Metastasis, Oral Treatment

1. Introduction

Breast cancer is a heterogeneous disease and the second leading cause of cancer death globally, involving one in every eight to ten women [1] [2] [3]. As a thought among novel research, the response could be in oxidative stress stories [4]. Oxidative stress phenomena may be due to low antioxidants or an excessive increase in the production of free radicals in the body. Chemical compounds and reactions capable of producing reactive oxygen species (ROS) are called pro-oxidants. Excessive reactive (ROS) formation can induce oxidative stress, leading to cell damage resulting in cell death. Therefore, cells have antioxidant networks to cleanse excessively the produced ROS. On the other hand, compounds and reactions that eliminate these species or suppress their production are referred to as antioxidants. There is a balanced ratio of pro-oxidants and antioxidants in a healthy cell. Nevertheless, this balance can be upset due to a decrease in the number of antioxidants or the overproduction of pro-oxidants following certain chemicals or medications. This condition is called oxidative stress. Oxidative stress and DNA damage (both mitochondrial and nuclear) is commonly defined as a cellular redox imbalance between oxidants and their precursors, which damages lipids, proteins, and nucleic acids [4] [5] [6] [7]. In the empire of nanoparticles (NPs), including carbon-based NPs, ceramic NPs, metal NPs, semiconductor NPs, polymeric NPs, and lipid-based NPs, where unique mechanical and physicochemical properties such as high surface-to-volume ratio (producing a reactive contact surface), the strategy of functionalizing, and impressive quantum effects, have no limit in creativity, there could be a solution against oxidation states. We strongly believe that zinc oxide NPs and their quantum dots due to their biosafety [8], biocompatibility [9] [10], heat absorbance [11], magnificent catalytic [12] [13], semiconducting [14], piezoelectric [15], magnetic properties [16], and surprisingly antibacterial activity [17], will be truly a promising platform for nanomedicine's novel discoveries. Looking back to the oxidative stress theory in the category of nanodrug mechanisms in the treatment of various cancers, which most nanotechnology scientists in this field consider, it should be noted that not all mechanisms of nanodrugs/nanomedicines can be summarized in this theory. In fact, besides oxidative issues, there is a new need to pay parallel attention to other topics such as the following key points: high

strength of NPs' permeability, produced interfacial chemical reactions between NPs and amino acids of subcutaneous proteins in times of injection into the body, and also the formation of strong hydrogen bonding bridges between the free electron pair of nitrogen and oxygen atoms of polar aqueous fluids and the electron oxygen pair of zinc oxide NPs in nano-solution. On the other hand, NPs conduct chemical reactions strangely/smartly in the environment around the spread of cancer cells, which cause the least damage to healthy cells (experience has shown).

As we need the suitable level of toxicity power of NPs against cancer cells, think carefully that the key factors in assessing the risk after exposure to NPs can be mainly particle size [7], effective surface area and their functionalized properties, suitable concentrations [18] [19], solubility in water, stability against sedimentation, and selection of new synthesis methods in the production of efficient NPs and quantum dot NPs with special properties of hydrophilicity and hydrophobicity. Unfortunately, the molecular mechanisms involved in the toxicity effects of NPs against cancerous cells are not yet fully understood, but researchers have shown that reactive oxygen species (ROS) play an important role in such effects. ROS factors are involved in the modulation of cell survival, cell death, differentiation, cellular signaling, immune systems, inflammation-related factor production, and cause severe damage to cell molecules, including protein, fat, and DNA, and have detrimental effects on the cells [20] [21] [22] [23]. Biologically significant ROS elements include free radicals, such as singlet oxygen ($^1O_2$), superoxide ($O_2^{\bullet -}$), and hydroxyl ($HO^{\bullet}$), which contribute to the generation of a non-radical and higher stability of H_2O_2 compound. High ROS levels and toxic hydrogen peroxide lead to nucleic acids, lipid oxidation and peroxidation, resulting in cellular apoptosis and necrosis. Superoxide production and H_2O_2 can constitute a key antioxidant defense in nearly all cells exposed to oxygen [16]. Notably, free radicals are produced from the surface of NPs when both the oxidants and free radicals bind to the NPs' surface. In addition, reduced NPs size results in various structural defects, including oxygen-deficient regions, trapping states, crystal defects, electron–hole pairs, etc., which can alter the electronic properties of the NPs surface, thereby the creating of "even more unique" reactive site groups [8] [24].

Regarding animal model trials, human tumors metastasize poorly in mice, and when metastasis occurs, unexpected features are often observed. In contrast, mouse tumor cells with a natural immune system are more effective at metastasis, with characteristics similar to those observed in cancer patients [25]. Since the immune system plays an essential role cancer development and progression, models that can be used in fully immunized mice will be extremely helpful in analyzing cancer progression and metastasis of cancer and evaluating drugs. So far, there have been few mouse models which can show bone marrow metastasis [26]. Mouse tumor cell line (4T1) is one of the several breast cancer cell lines which can metastasize effectively to areas with infected human breast cancer

[27]. The 4T1, derived from a spontaneous tumor in BALB/c mice, can metastasize to several organs involved in breast cancer, such as the lung, liver, brain, and bone. These cells have been used to develop several immunotherapies [28] [29]. Based on extensive past experiences [8] [14] [17] in producing effective nanomedicines against various cancers, zinc oxide NPs and ZnO Q-Dot NPs were used as the main base in this research. These NPs were fabricated by modern methods in nanotechnology, including the sol-gel method, cold and heat fast-quenching technique, professional and new hydrophilic surface modification and hydrothermal procedures. These compounds were then formulated with zinc oxide nanopolymer ZnO@PVP as co-assistant in an effective nanofluid, including solubilizer and wetting agents ethoxylated, PEG-bonding agents (polyethylene glycol), and water-in-oil emulsifiers sorbitan in the polar and eco-friendly solvent. Complete characterization was performed, and animal model tests were carried out on BALB/c mice using high-risk 4T1 breast cancer cell lines. At this stage, intraperitoneal, intravenous injection and oral tests were performed thoroughly and fortunately, the results were reported positively in all steps and the appropriate dose was determined. Eventually, due to the histopathological symptoms, all the tumor masses that had formed and grown in the cancer mice completely disappeared, and no metastases were seen in their organs after nine months of treatment. In addition, the newborn mice were perfectly healthy. Importantly, this research is ready to be tested on volunteer breast cancer patients in life-threatening situations.

2. Material and Methods

2.1. Cell Culture

The cell line (4T1) of the breast (adenocarcinoma mouse) was obtained from the Pasteur Institute of Iran. The cells were stored in a high-glucose DMEM medium containing 10% fetal bovine serum, 5% non-essential amino acids, and the Penicillin and Streptomycin antibiotics in a 37˚C incubator containing 5% CO_2 to obtain the appropriate number. Six weeks after starting the research protocol, 1×10^6 cells were injected subcutaneously into groups assigned to the tumors. The tumor was palpable in animals about two weeks after injection. Tumor volume was measured in two longitude and transverse axes. The largest dimension of the tumor was the length (L), and the other dimension (at a 90-degree angle) was considered the width (W). Once every two days, the length and width of the tumor were measured by a caliper and the tumor volume introduced by Jones *et al.* 2010, was calculated using the following formula [30], [$V = 1/2(L2 \times W)$].

2.2. Experimental Animals

To evaluate the antitumor effect of ZnO quantum dot NPs/nanodrug, Female BALB/c mice (22 - 24 g, 6 - 8 weeks of age) were maintained in cages at 22˚C ± 3˚C, 55% relative humidity of under a 12-h dark/light cycle. Mice were allowed free access to food and water. After 12 days of tumor induction, the animals

were randomly divided into ten groups of seven. This research has been done in animal labs as Balb/c mice in ZFP (Zist Faravard Pars, Tehran, Iran) company based on moral code (ethical principles).

2.3. *In Vivo* Tumor Treatment Studies

Mice were divided into four control groups (n = 10) and three treatment groups (n = 10). The first treatment group used zinc oxide nanodrug with concentrations of 20, 40, and 60 μg/ml daily with a volume of half a cc using an insulin syringe intraperitoneally, while the second treatment group received an injection (intravenous pyelogram, IVP), and the third group was treated orally. The group control was injected with half a cc of deionized distilled water. Mice were killed and studied four weeks after injection. The control group used only normal water and compressed rat food (pellets) during this period. Compacted mice food (pellets) containing substances such as soybean meal, corn, wheat bran, and fish meal with pure protein, fat and fiber contents of 22%, 2%, and 3.3%, respectively, and sufficient amounts of vitamins, sodium chloride, calcium carbonate, and calcium phosphate, obtained from Pars Daneh Company Kermanshah, Iran. The amount of food given was weighed for 24 hours in each group and after 24 hours, the remaining food was weighed. The food consumption in each group was calculated using this difference. In the treatment groups, vitamin C (500 mg/500ml) was added to the diet with food. It has an influential antioxidant role, is vital for the immune system and neutralizes free radical molecules. Mice were examined daily for physical and behavioral characteristics.

2.4. Blood Collection

The distal one-half centimeter of the tail was clipped, and a capillary pipette containing anticoagulants (EDTA for cell counting was used to collect a 5 ml sample from the bleeding surface). The sample was used for cell counting. Immediately after collection, the cut surface of the tail was cauterized with styptic powder (Kwik-stop, ARC Laboratories, Atlanta, GA) [31] [32].

2.4.1. Sample Processing

White blood cell count (Leukocytes)

Blood sampling was performed at week 1. The number of leukocytes was calculated using the modified Klonz. Calculation of leukocyte amount was performed by using a Thoma leukocyte pipette. Blood samples treated with anti-coagulant were smoked with pipettes until the "0.5" mark. The pipette was then immersed in the Rees-Ecker solution and inhaled until the "11" sign to obtain a 1:20 dilution. The pipette is flipped for about 3 minutes by forming a quarter of the circle; then the first 2 - 3 drops of blood are removed. Furthermore, the blood drops on the side of the counting room at an angle of 30˚. Room count is allowed one minute, which aims to lyse erythrocytes and give leukocytes a chance to occupy the count room. The leukocyte amount was performed with a 40× magnification microscope on four large boxes of count chambers. The

number of leukocytes per cubic millimeter (mm^3) is the number of calculated cells multiplied by 50 [33].

2.4.2. Slide Preparation

Blood samples without EDTA were dripped on the object glass and smeared using the right hand placed another object in front of the blood drops at an angle of 30˚C - 40˚C. The second object, glass, was pushed forward to form a thin smear. To examine and count the blood cells, a drop of blood was obtained from the mice under study. After drying, the smear is fixed with methanol for 3 - 5 minutes and allowed to dry in the air. The preparations are then stained with Giemsa's solution with 1:9 dilutions for 30 minutes (phosphate buffer pH 6.8 - 7.2). The preparations were then washed with aquades and allowed to dry on the shelf. After dry preparations are examined under a microscope with 100× magnification, each type of leukocytes (white blood cells, WBC) is calculated by battlement method, using a blood counter tabulator. Interrupted count of at least 100 cells and calculated the percentage of leukocyte types (they are classified into two main groups: (granulocytes and nongranulocytes). The granulocytes, which include neutrophils (play a major role in the early defense of non-specific immunity against bacterial) infections, eosinophils (play a role against parasitic and allergic diseases), and basophils cells (to prevent freezing and static blood and lymph by heparin) and the nongranuloctye white blood cells are lymphocytes (play a role in the immune response) and monocytes (are the largest cells in the periphery with blue-grey ground glass cytoplasm). The number obtained is the relative amount of each leukocyte type from all leukocytes [34].

2.5. Measuring Lipid Profile (Cholesterol Index)

Blood samples were taken using capillary tubes from the inner corners of the animal's eyes. The drawn blood was centrifuged at 3000 rpm for 15 minutes to separate the serum from the clot. Finally, the serum lipid profile was assessed using Pars Azmoon Co. (Iran) kits.

2.6. Anesthesia, Weighing, and Sampling of the Animals

In this study, the mice were weighed before killing and then anesthetized with ether. Under the hood and sterile conditions, the skin of the abdomen and spleen was opened, and the area of the breast tissue with the tumor was isolated and kept in 10% formalin for pathological study.

2.7. Histopathological Examination

For histopathological examination in mice, biopsies were taken from the breast tissue of the treated mice after the morphological examination. Samples prepared after fixation in 10% formalin solution underwent dehydration, clarification, and impregnation for paraffin molding. After preparing paraffin molds from the samples, 6 µm sections were prepared, stained by the hematoxylin and eosin (H&E) method and examined for histological changes using an OLYMPUS-

BX51 microscope.

2.8. Histological Study by Hematoxylin-Eosin Staining

At this stage, tissue processing, molding, and preparation of paraffin blocks were performed by a pathology technician in the research center of Pars Bioproduct Company and 4 μ thick sections were prepared by microtome. To confirm the presence of tumor tissue in tissue sections, sections were prepared for hematoxylin and eosin staining, and the quality of the incisions was evaluated before and after tumor diagnosis and grading. To stain hematoxylin and eosin, the slides were first kept in an oven for 1 hour, transferred to 3 xylenol glass containers where they were kept for 5 minutes, dried and then placed in 3 containers of 96% alcohol in which they were washed for about 1 to 2 minutes. Next, the slide was immersed in hematoxylin, alcohol, sodium acetate, and eosin for 7 minutes, 2 seconds, 1 second, and 2 - 3 minutes, respectively, and washed between these steps. Finally, the slides were placed in 3 containers of 96% alcohol each and dried for a few seconds, followed by adding a few drops of xylenol. Finally, coverslips were placed on the slides. The stained parts were graded according to the degree of the tissue abnormality, which was scored with the following five parameters as the characteristics of breast dysplasia and neoplasia:

1) Core to cytoplasm ratio (50% <: 2, 25% - 50%: 1, 25% > :0)

2) Epithelial stratification (0: monolayer coverage and lack of stratification, 1: moderate stratification, 2 severe stratifications)

3) Lack of nuclear polarity (0: suitable nuclei polarity, 1: medium nuclear polarity, 2: completely disordered polarity)

4) Reduction of goblet cells (0: normal goblet content, 1: moderate absence of goblet cells, 2: severe lack of goblet cells)

5) Structural anomalies (0: preserved structure, 1: Moderate disruption, 2: Severe disruption)

3. Results and Discussion

3.1. Weight Changes

The weight of each rat in the study groups was determined. To do this, the weight of the groups was measured daily after two weeks of cancer cell injection. The mean weight of the mice in the four groups did not show a statistically significant difference. The mice in the control group and those treated with nanodrug weighed 21.20 ± 0.78, 21.09 ± 0.21, and 21.68 ± 0.68 grams, respectively, after injection.

3.2. Differential Count of Peripheral Blood Leukocytes

Spread was prepared from the peripheral blood of the animal and stained by the Giemsa method (a nucleic acid stain used in cytogenetics and for the histopathological diagnosis), followed by the differential counting of leukocytes, the results of which are reported as a percentage in Table 1 and Table 2 and S11-S12

(in Supplementary Data). Table 1 shows the animal model's three important white blood cell types (lymphocyte, neutrophil, and monocyte) for 20, 40, and 60 (μg/ml) nanodrug concentrations. The methods used in Table 1 are intraperitoneal, injection into a mouse tail vein and oral, which were compared with the control group. Lymphocytes are produced in the bone marrow and play an important role in fighting cancer and infection. They are an important part of the immune system. Neutrophils (also known as neutrocytes or heterophils) are a type of white blood cell that act as your immune system's first line of defense. A low neutrophil count (neutropenia) leaves your body more open to infection. Moreover, if an infection occurs, the body may be unable to fight it. Monocytes are responsible for attacking and breaking down germs and bacteria that enter the body.

Table 1. Blood cell count results in the nanodrug receiving groups and control.

Groups	Nanoparticle concentration (μg/ml)	Blood parameters		
		Lymphocyte (%)	Neutrophil (%)	Monocyte (%)
Intraperitoneal nanodrug receiver	20	57	39	4
	40	58	40	2
	60	56	41	3
Injector nanodrug receiver	20	56	41	3
	40	60	38	2
	60	57	40	3
Oral nanodrug receiver	20	59	38	3
	40	54	44	2
	60	57	40	3
Control		**58**	**40**	**2**

Table 2. Measurement of blood cholesterol index in the control group and the group receiving nanodrug.

Groups	Nanodrug concentrations (micrograms per milliliter)	Serum cholesterol level (mg/dl)
Intraperitoneal nanodrug receiver	20	198
	40	187
	60	156
Injector nanodrug receiver	20	207
	40	143
	60	140
Oral nanodrug receiver	20	201
	40	**99**
	60	102
Control		**582**

This study examined and evaluated several factors and important variables in the animal model. These variables were: consideration of animal weight before and after receiving the nanodrug, measuring the tumor created in terms of weight, length and width., evaluation and counting of white blood cell parameters at three selected concentrations of nanodrug along with three methods used in the study, assessment and measurement blood serum cholesterol level after receiving nanodrug, examination of animal histopathology after recovery by nanodrug and observation of changes in tissues of animal body parts after recovery by nanodrug. Of course, tumor markers such as Tumour Necrosis Factor-alpha (TNF-alpha) could be evaluated to assess the level of safety of the animals under study, but this was not possible in this study, and its investigation was postponed to another time. From the study and experiments in **Table 1**, it was observed that: regarding the parameters of white blood cells in the desired test conditions (three different methods, three various concentrations, and three diverse groups of blood cells), there was no remarkable change in the count of blood factors compared to the control group. Furthermore, the obtained numbers did not show a significant difference. In other words, changes in nanodrug concentration in **Table 1** had no significant effect on blood parameters (except in neutrophil and lymphocyte). As a result, no effective data were achieved from this experiment. However, it still is important to have these data.

In **Table 2**, serum cholesterol levels were measured compared to the control group, according to three different procedures, along with three concentrations of nanodrug. Based on the results of this work, and in connection with the measurement of blood cholesterol, it can be concluded that the use of produced nanodrug for challenged animals, with different used concentrations as well as the various methods, was shown to be a very effective impression in reducing serum cholesterol levels compared to the control group. This interesting effect of the concentrations factor worked much better. Herein, the 40 μg/ml concentration compared to other concentrations in the table showed a significant decrease. Another great point that can be deduced from this study is that the oral method has shown the best results compared to other methods (our goal was to find the best method at this concentration).

3.3. Scientific and Essential Points about Cancer

According to this paper's extensive and valid research, this work aims to provide logical and advanced answers to some questions including, 1). What are the effects of nanomedicine in the body of cancerous breast mice and their grown gland [35]? In this perspective, what happens in the metabolism of the cancerous mice [36]? 2). How does the nanomedicine react with the body of a cancer patient [37]? 3). What are the first reactions of cancerous glands to nanodrug [38]? Do they change in size, and why do they disappear? 4). According to modern biological theories or biochemical or chemical science, why does the growth of cancerous glands stop by cancer nanomedicine [39]? 5). When do cancerous

glands grow and what complex and unknown physiological fluids are produced in the environment around cancerous glands, which distinguishes them from other normal cells? This situation causes the tumor to grow and spread, and the NPs are intelligently attributed to it, absorbed, and accumulated preferentially in the carcinoma tumor tissue [40] [41]. 6). Finally, from a biological point of view and specialized nanomedicine, what is the mechanism of action of nano-based drug delivery systems for breast cancer tumors? It is likely that with the advancement of nanotechnology knowledge in the vast medical science, nanotechnologists will be able to respond to all these helpful questions in the near future. Indeed, a team of biological scientists, geneticists, biochemists, and chemists can support nanotechnologists in answering these unknowns.

3.4. Histopathological Results

Histological analysis studies the microscopic anatomy of cells and tissues of organisms. In the posterior region and the midline of the mice body in the control group and the group treated with nanodrug product, a mass of several centimeters was observed, which was not present in the group treated with nanodrug product. During treatment, the size and weight of the tumors decreased and, interestingly, after two weeks of treatment, they completely disappeared. Nanodrug oral treatment treated a larger population of cancer mice than other expressed methods and showed better response. After sampling the mass and performing the stages of preparation of tissue sections and Hematoxylin/eosin (H&E) staining, the samples were examined under an optical microscope. Both samples had abundant mitotic divisions and atypical cells, including bizarre cell formation. According to the shape of the photomicrographs of histological analysis, only the control group had an anaplastic tumor mass (**Figure 1(a)** and **Figure 1(b)**). Anaplastic large cell lymphoma (ALCL) is a rare T-cell lymphoma that expresses the lymphocyte activation marker CD30 that can involve the breast. Histological particular types of breast cancer are preferentially oestrogen receptor positive or negative. According to the literature, the oestrogen receptor is probably the negative type in this study. Histopathological analysis of tumors can visually examine the regularities of cell shapes, size, tissue distributions, cancer detection and grading applications. **Figure 2(a)** and **Figure 2(b)** illustrated a thin slice (section) of tissue under light (optical) or histology images for the oral group treated with the nanodrug product. Consequently, the nanodrug product was impressive regarding the histopathological symptom results. Hence, all the tumor masses that had formed and grown in the cancer mice completely disappeared after two weeks, especially in the oral method, and no metastases were observed in their organs after nine months of treatment and maintenance in completely standard conditions. Finally, this phenomenon was one of the critical points of *in vivo* research by a newly synthesized nanomedicine product. These histology images are regarded as the gold standard for the clinical diagnosis of this study and the identification of prognostic and therapeutic targets.

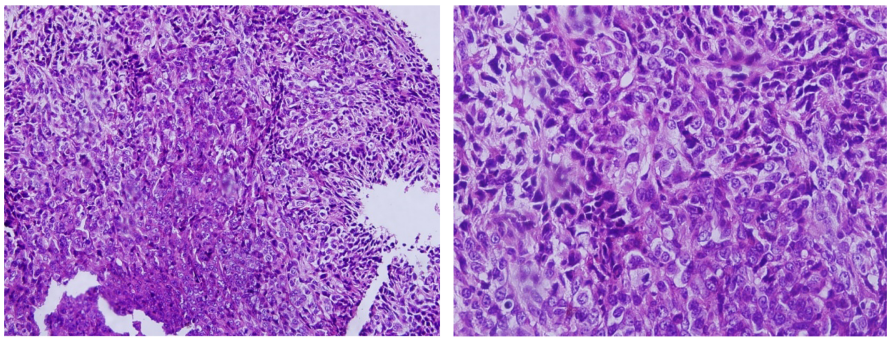

(a) (b)

Figure 1. Cross-sectional photomicrograph of a tumor mass belonging to the control group and the presence of numerous scattered mitotic divisions and atypical anaplastic large cell lymphoma, including bizarre tumor giant cell formation, H&E staining in (a) 200 and (b) 400 magnifications. Atypical medullary carcinoma (type A) is syncytial architecture with a high nuclear grade, no glandular or tubular structures and diffuse lymphoplasmacytic infiltration.

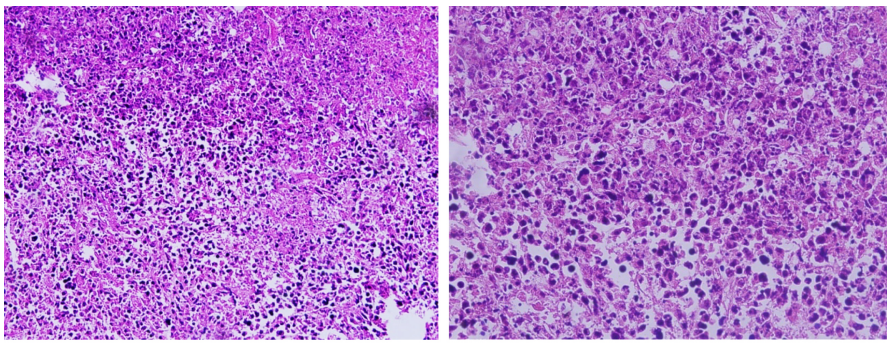

(a) (b)

Figure 2. Demonstration of photomicrographs of histological sections of the therapeutic phenomenon of cancerous tumor masses. These are specific to those mice that were treated orally with nanodrug. Photomicrograph shapes showed different histological images of the control groups. H&E staining images can also be seen at (a) 200 and (b) 400 magnifications.

As mentioned earlier, the oral nanodrug product was successfully treated malignant breast cancer masses so that the sick mice recovered completely and no metastases were observed after nine months under standard care. Interestingly, no signs of tumor spread were observed at the end of treatment. In fact, they had disappeared entirely.

3.5. The Empirical Conclusion of the Animal Model Section

Studies have shown that using the 4T1 cell line can be useful for studying late-stage breast cancer and evaluating cancer nanodrugs and other therapeutic compounds [42] [43]. Miller and colleagues first obtained this cell line at the Karmanos Cancer Institute from a breast tumor that developed spontaneously in BALB/c mice [27] [28] [29] [44] [45] [46] [47]. In our interesting and professional work, a strong nanomedicine was synthesized based on two effective na-

nomaterials: ZnO Q-Dot NPs and a ZnO@PVP nanopolymer, which various chemical effective agents formulated in a polar and water-based solution. This final nanoproduct (nanodrug) was very stable and water-soluble without agglomeration with unique physical and chemical properties. The toxicity of this nanodrug, which was used for *in vivo* tests on mice in this study, had previously been thoroughly investigated in the laboratory [8] [14]. Hence, the US Food and Drug Administration (FDA) has classified ZnO NPs as a "GRAS" (generally) regarded as a safe substance [48] [49] and is considered safe both in *in vitro* and *in vivo*. Also, they can act as nanocarriers for tumor-targeted medication administration and potent anti-cancerous agents. The experimental section fully discusses the fabrication and characterization of this compound. In the following study, the nano-treated mice were divided into treatment group 1 and treatment group 2. In treatment group 1, a known dose of the nanodrug was injected directly into the throat of a mouse (so-called "forced and programmed oral feeding") (nanodrug code 1). In this method, cancerous mice were fed a mixture of water@nanodrug regularly and at a specific time (programmed-compulsory method). In treatment group 2 (nanodrug code 2), the same nanodrug with the same concentration was added to the mice drinking container, and the mice drank the solution irregularly and efficiently (so-called "optionally eaten"). This method involved random drinking and did not have a set time. Thus, different mice might drink different amounts of water. Of course, this innovative treatment method was not ineffective. Both oral methods successfully treated mice during two weeks (for code 1) and four weeks (for code 2) at a given dose, but the tumor glands disappeared completely in both groups. A larger population of mice treated with nanodrug code-1 became healthy and safe. According to all the results of the studies conducted in this part of the animal model research, including biological, cytological, hematological, anatomical, and histopathological studies, mice with breast cancer were treated using an effective nanodrug containing zinc oxide Q-Dot NPs, and the desired materials could completely cure breast cancer. It also prevented metastasis to other tissues and organs in the studied mice at the dose of 40 μg/ml in a two weeks course of oral administration compared with the control mice. However, in various experiments performed by different methods (intraperitoneal, intravenous injections, and oral), no traces of tumor masses were observed in mice with breast cancer in the multiple tests mentioned above. Subsequently, the replication process of the animal model was performed only orally, and no traces of proliferated tumors and metastases were observed in the mice receiving the nanodrug in a controlled manner. Thus, these findings imply that ZnO Q-Dot NPs and their nanodrug could be the best candidate for fighting breast cancer. In ordinary cells, there are constant signals which determine their behavior. This means the cell must divide into multi-cellular organisms, lead to characteristic cell changes (morphology), enter another cell, or eventually die (molecular mechanisms of programmed cell death-apoptosis). Although heredity is involved in only five to ten percent of

cancers, other causes, such as poor diet, certain infections, inactivity, obesity, smoking, and direct or indirect contamination, can affect the activity of certain genes and the growth rate of cancerous glands. NPs can easily interact with biological molecules, manipulate different cell cycles, and clearly affect homeostasis. It seems that these NPs have a great activity in inducing gene expression. As potential chemicals, they can prevent the development of breast adenocarcinoma. NPs with significantly smaller diameters are suspected to be able to enter tumor cells more easily, thereby stimulating the biological response more effectively. Our results showed that in mice with breast cancer caused by the 4T1 cell line, tumor growth was effectively inhibited by this new nanodrug diet. The therapeutic response to treatment with this formulated nanodrug was determined through physical examination because fewer tumors were palpable in this group of mice. In addition, examining the images of tumor tissue biopsies after treatment with our nanodrug showed that breast cancer had slower growth in mice treated with nanopharmaceuticals. In contrast, in the other groups (controls), different regions of abnormal cell proliferation were formed, indicating the rapid development of cancer. In addition, according to microscopic slides, the peripheral blood spreads of the examined mice showed an increased presence of lymphocytes. These lymphocytes' presence can be a very favorable prognostic factor in the removal and destruction of cancerous glands. The findings indicate that this nanodrug can produce cytokines such as tumor necrosis factor-alpha (TNF-α), an important factor for resistance to infection and cancers [50] [51]. Importantly, authors have reported that cytokine production increases after the mice are exposed to the inhalation of zinc oxide nanodrug. In addition, cytokines enhance the immune development induced by cytotoxic cells, which may increase tumor targeting and growth inhibition. Based on the microscopic observations of this study, *in vivo* treatment with nanodrug may potentially activate the natural immune response against adenocarcinoma at the selected dose. Since chemotherapeutic agents may have an even wider range, applications in the treatment of cancer cells, dosage, particle size-dependent activity against cancer cells, and changes in toxicity are among the factors, which should be examined more frequently. It is hoped that the acceptable and effective results of this research can be very promising for the pharmaceutical and medical industry and used in the treatment of human volunteer patients with acute breast cancer without any side effects as a practical step in treating such patients. On the other hand, this new nanodrug can be used orally without any stress of drug injection, anticancer therapies, chemotherapy, radiotherapy, and radiation therapy. **Figure 3** shows the process of the practical application of an animal model using a new nanodrug for the treatment of breast cancer.

In this Figure, it can be seen that after the standard conditions for providing cancerous laboratory mice, and the intense growth of tumors that were observed. Mice were treated in three ways, whereas our standard gold point was to use the oral method. Challenged mice became healthy and pathological with

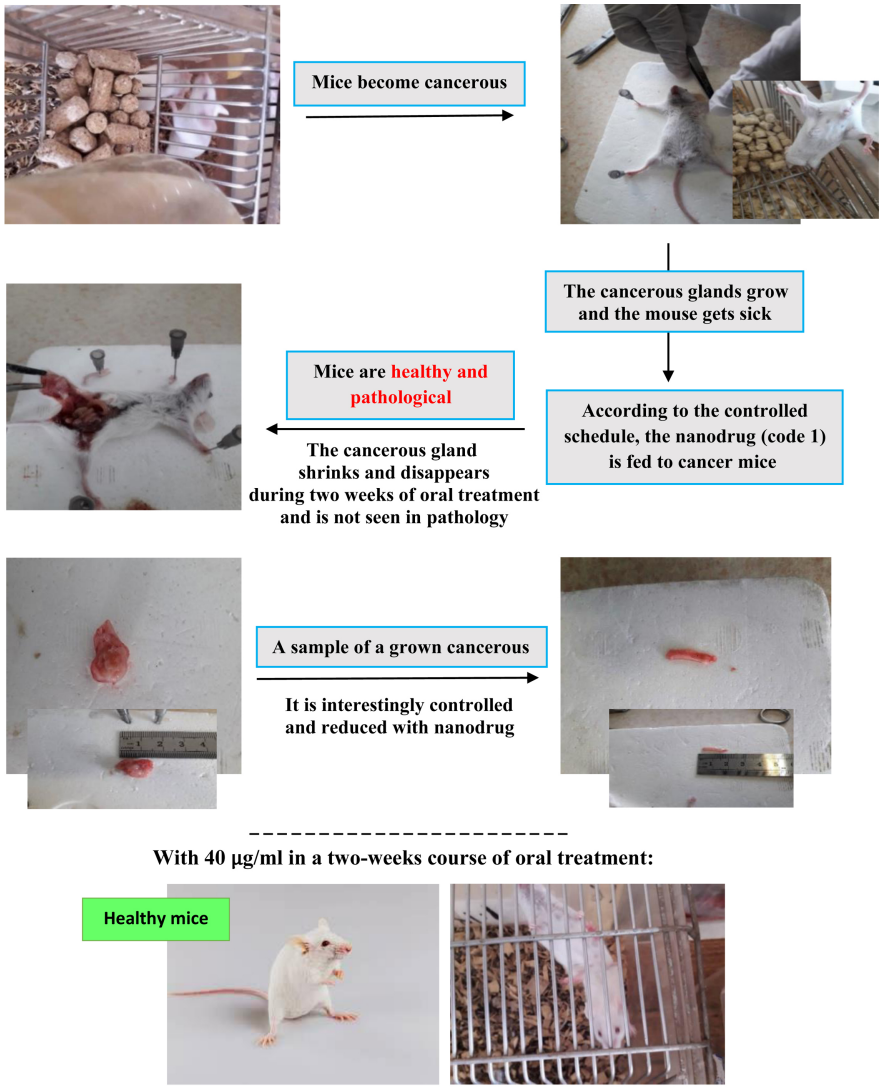

Figure 3. Executive steps of research on the application of nanomedicine in an animal model of breast cancer treatment.

daily nanodrug treatment, being always compared with the cancer tissues of the control groups. In the control groups, the cancerous tumor was large and developed, while the cancerous tissue in the treated ones was reduced entirely and disappeared. After 14 days, the healthy mice started to move and jump again in their cages and were well fed. The complete process of these healing steps can be seen in supplementary data.

3.6. Synthesis of Novel Nanoformulation Fluid Product (Nanodrug)

3.6.1. Synthesis of Hydrophilic ZnO Q-Dot NPs as the Main Basis of Nanodrug

17 - 19 gr zinc acetate. $2H_2O$ (Sigma Chemical Co., St. Louis, MO) solution was alkali hydrolyzed with pharmaceutical hexamethylenetetramine through sol-gel, wet-chemical synthesis (as modification of the precipitation method), and hy-

drothermal methods [8] [14]. In order to reduce the size of zinc oxide NPs to very small and fine, special chemical cold and thermal shock methods were used in the synthesis process (as Fast Quenching Conditions). On the other hand, for the fine NPs to dissolve well in water and water-based solvents and eliminate their toxicity, the surface of the NPs must be hydrophilized. In this regard, 7 - 9 gr of green carbocyclic fatty acids such as soybean fatty acid or oleic acid were added. The mixture was heated to reflux by coprecipitation/hydrothermal method that the surface of the synthesized zinc oxide NPs was completely hydrophilic [52]. Surface coating is a suitable method for preventing the aggregation of NPs. The pH of the solution was adjusted in the range of 9 - 11; the reaction mixture was then refluxed for 12 hours and finally dried in an oven at 80˚C for 8 hours (zinc hydroxide is converted into ZnO NPs by calcining at 80˚C). The zinc oxide NPs is the important and very strong and energetic base of quantum fine NPs, prepared in this way. Fatty acid and organic amines are the most common stabilizers used to coordinate with Zn atoms on the surface of ZnO Q-Dot NPs to hinder the formation of bulk ZnO [53]. This part of our work was registered as a patent in Iran in 2014 for the *in vitro* treatment of breast and colon cancers. **Figure 4** shows the chemical pathways of ZnO NPs process through alkali hydrolysis of zinc acetate and $2H_2O$ salt without the added fatty acid and surface modifying agents.

3.6.2. Synthesis and Fabrication of Nanopolymers (PVP-Capped ZnO NPs) as the Second Base of Nanoformulation Product

In order that zinc oxide Q-Dot NPs can fight against dangerous cancer cells in the human or animal body, they must be stable enough to penetrate and not decompose with stomach acid. It is necessary to have a strong nanopolymer that fully supports this. For this purpose, 3 - 4 gr of non-toxic and biocompatible polyvinyl pyrrolidone (PVP) were converted into a strong nanopolymer by coprecipitation, hydrothermal and fast quenching methods using zinc oxide NPs [14] [53]. According to a study, PEG-coated ZnO NPs are considered more stable than ZnO NPs alone [48], with low damage to normal cells compared to naked ZnO NPs. In this procedure, a very small amount of zinc oxide NPs (0.5 - 1 gr) in a solution of water and alcohol and a mixture of a stabilizer and a suitable ethoxylated alcohol surfactant were chemically reacted with PVP polymer. The

$$Zn(CH_3COO)_2.2H_2O + 2KOH \rightarrow Zn(OH)_2 + 2CH_3COOK + 2H_2O$$

(Alkali hydrolysis by KOH at suitable pH according to isoelectric point of ZnO NPs at 9–10, and formation of acolloidal–gel of zinc hydroxide) – sol reaction.

$$Zn(OH)_2 + 2H_2O \rightarrow Zn(OH)_4^{2-} + 2H^+ \text{ (colloidal–gel of zinc hydroxide)}$$

$$Zn(OH)_4^{2-} \leftrightarrow ZnO + H_2O + 2OH^- \text{ (pH controls the rate of ZnO formation, size and stability of ZnO NPs).}$$

After removing water at 80 °C, this gel convertsto final product of ZnO NPs.

Figure 4. Chemical KOH hydrolysis processes for the fabrication of ZnO NPs with wurtzite structure, hexagonal phase, and n-type semiconductor.

reaction mixture with vigorous stirring was refluxed for 10 hours and kept in an oven at 80˚C for 48 hours by hydrothermal method. The nanopolymer was prepared in a mixture of monopropylene glycol (MPG) solvent and formulated as a dispersant along with nonionic surfactant sorbitan monooleate, Span 80 as a W/O emulsifier at room temperature. The surface of nanopolymer is modified and made hydrophilic by this method.

3.6.3. Production of a Water-Based Nanofluid Formulation as the Final Anticancer Agent (Nanodrug)

First, 1 - 3 gr of the zinc oxide Q-Dot NPs were dissolved in 10 ml of distilled water. 2 - 4 g of ZnO nanopolymer were then dissolved in 10 ml of distilled water and added to the first product and the mixture obtained was stirred at 40˚C and completely dissolved. To prepare the formulation, 4 - 5 ml of a solution of 8 - 10 moles of ethoxylated alcohol surfactant (as a wetting agent) (Kimyagaran Emrooz Chemical Company) were added, and the obtained product was kept in an ultrasonic bath for 2 - 3 hours. To make the obtained nanofluid more stable, 2 - 4 gr of polyethylene glycol (PEG) with a molecular weight of 4000 - 6000 were used as an auxiliary solvent (binding agent) and nanofluid holder in water to make the final product more hydrophilic. Afterward, the pH of the solution was adjusted. Then 1 - 2 ml of a water-based emulsifier (W/O) of the sorbitan group (Merck Chemical Co., Darmstadt, Germany) were then added, and the resulting product was thoroughly stirred to become uniform and homogeneous. The resulting final nanoproduct was viscous, yellow in color, very stable and soluble in distilled water. On the other hand, this nanodrug is very active and has high permeability and diffusivity into the membrane between skin cells and the space around tumor cells. In applying ZnO Q-Dot NPs, Q-Dots must be water-stable [54] and in the form of a colloidal solution. Based on our extensive experiences, this sample has a large surface area (high BET), excellent safety by the US Food and Drug Administration, good biocompatibility, anti-bacterial activity, non-toxicity, and low cost. **Figure 5** shows the typical protocol for formulating a synthesized nanodrug animal model study. Chemical-physical and biological relationship between the main components (zinc oxide Q-Dot NPs and nanopolymer) in polar and aqueous solutions, the wetting agent, durable binding reagent, and a suitable emulsifier group in the regulated pH can produce a powerful and efficient nanopharmaceutical.

3.7. Apoptosis and Necrosis Analysis

In 2018, we analyzed apoptosis and necrosis in the *in vitro* studies section of the above anticancer nanodrug. We had worked completely and, in this article, due to its large volume, this analysis was not discussed. The death of a cell occurs in two different ways, namely apoptosis or programmed cell death and necrosis. Necrosis is a collection of dead cells and tissues at one point in the body. A blockage usually causes tissue necrosis in blood flow. Sometimes infections or chemicals can also cause tissue necrosis. Apoptosis is a regular process of cell

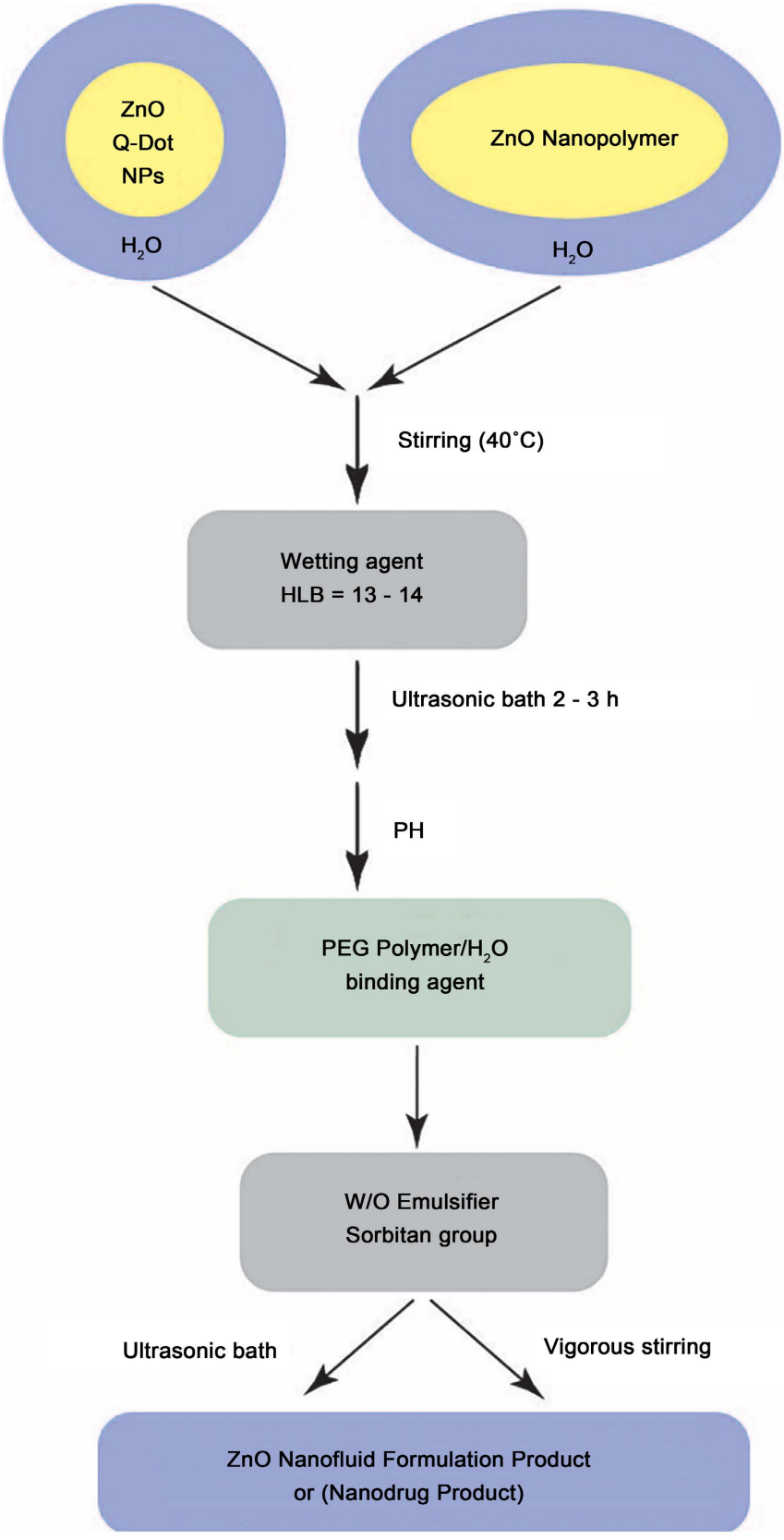

Figure 5. Demonstration of the preparation process of nanodrug formulation used in the animal model.

death in the body where the cell itself participates death. In this study, flow cytometry results showed that the apoptosis process in ZnO nanodrug treated MCF-7 cells revealed approximately the same percentage of early and late apoptotic cells (15% and 22%, respectively) within 24 h, while the proportion of MCF-7 cells went much higher after 48 h (up to 60%) [14].

3.8. Characterization of Various NPs in Nanoformulation Product

3.8.1. SEM Images of ZnO Q-Dot NPs and ZnO@PVP Nanopolymer

SEM (transmission electron microscopy) images with larger magnifications show the surface morphology and structure of zinc oxide Q-Dot NPs modified with green fatty acids (fine NPs of 1 - 3 nm size). They act like small atomic and have a very high permeability. The NPs are fully dispersed through the hydrophilic agent. Thus, these beautiful small NPs are located between eco-friendly green fatty carboxylic acid and nonionic ethoxylated template layers (**Figure 6**). In fact, the morphological surface of the modified ZnO Q-Dot NPs appears to form a mixture of small nanospheres and nanorods structures, surrounded by fatty acid groups. Thus, we can see spherical NPs and fine nanorods separately in **Figure 6** and this collection forms the overall structure of zinc oxide Q-Dot NPs.

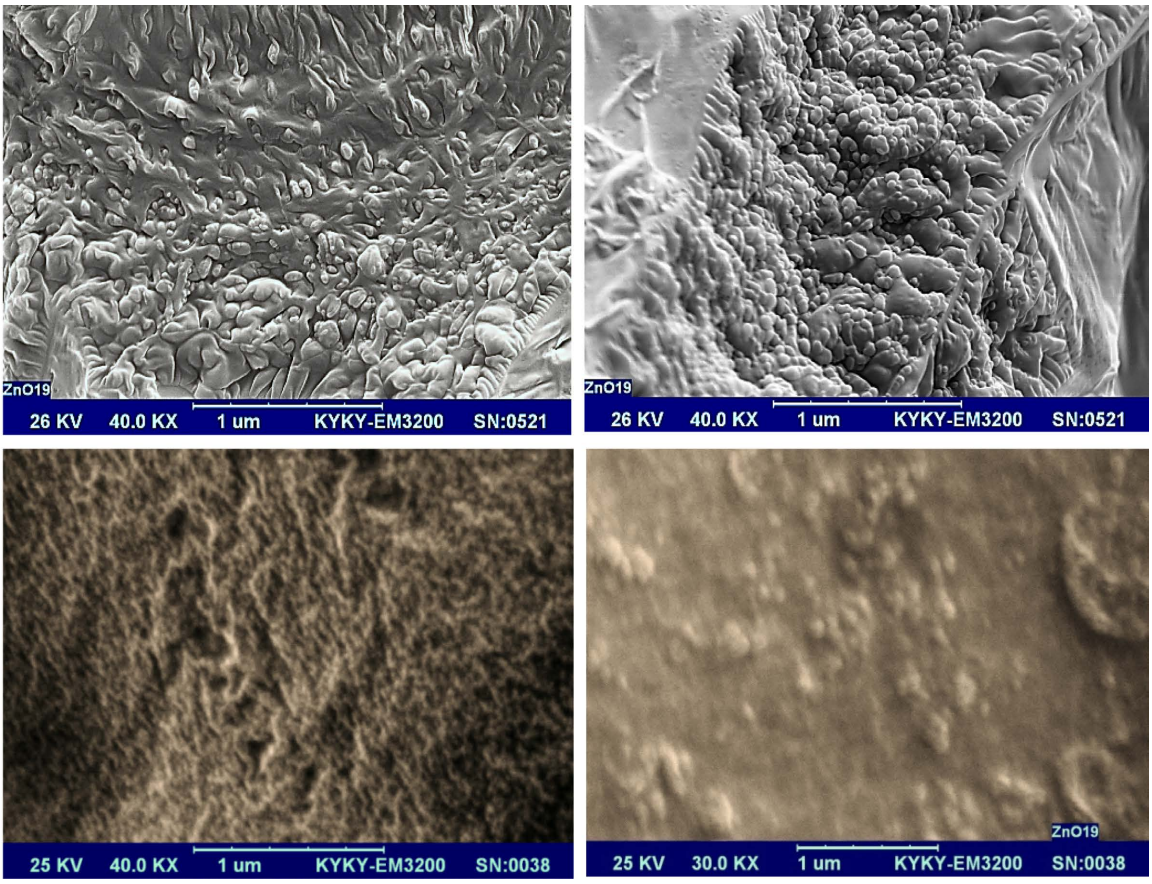

Figure 6. SEM (KYKY EM 3200) morphological images of surface modified ZnO Q-Dot NPs by various functions in the nanofluid formulation.

The SEM images of attractive ZnO@PVP nanopolymer as unique synergistic agents for ZnO Q-Dot NPs in nanofluid formulations are shown in Figure 7.

The role of these nanocomposites in attacking cancer cell lines is very serious and practical. They are very significant companions and valuable supporters for ZnO Q-Dot NPs. Nanopolymers appear to increase the attack activity of ZnO Q-Dot NPs on cancer cells. Because quantum dots have a unique structure and high permeability. In other words, they act as a synergistic process, and when the NP concentration is exhausted, the ZnO@PVP nanopolymer supports this mechanism. Perhaps these NPs attack cancer cell lines together. Of course, the exact mechanism of the attack on the cancerous glands is not yet known. However, experience shows that smaller NPs can move and attack cell membranes sooner.

3.8.2. Transmission Electron Microscopy (TEM) Study of ZnO Q-Dot NPs

Figure 8 shows transmission electron microscopy (TEM) micrographs (Philips CM30) of ZnO Q-Dot NPs functionalized by green vegetable carbocyclic fatty acid and various effective surfactants during the synthesis.

The average size of nearly monodispersed and crystalline zinc oxide Q-Dot NPs is very small. The SEM images (in SEM, nano spherical particles and nanorods have been immersed among the layers) show the lattice fringes between two

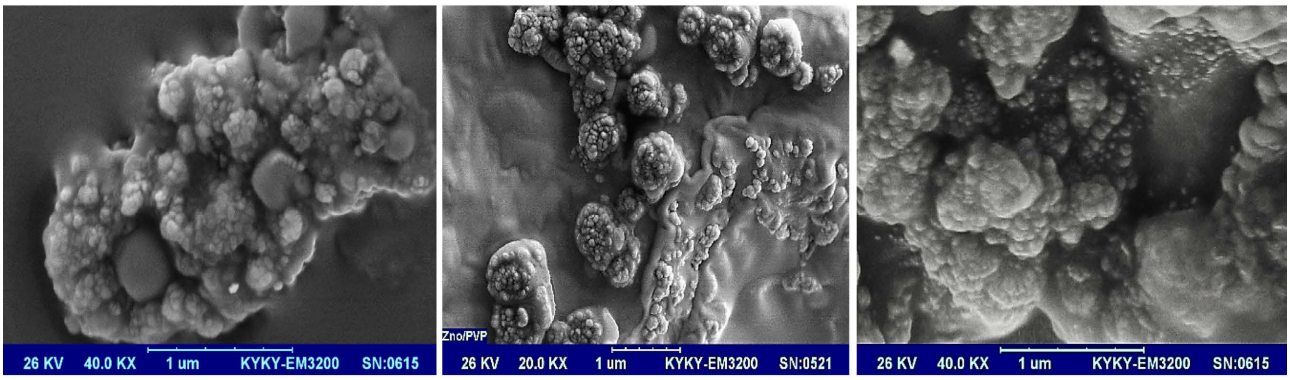

Figure 7. SEM (KYKY EM 3200) morphological images of ZnO@PVP nanopolymer created as homogeneous small spherical NPs in nanocomposite polymer at high magnifications.

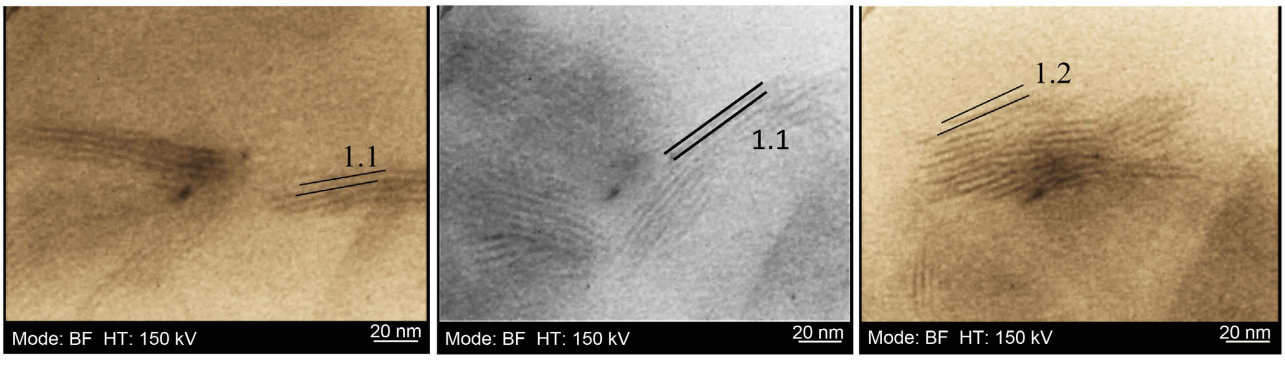

Figure 8. Typical high-resolution TEM micrograph of the ZnO Q-Dot NPs. Most measuring scales are between 10 - 20 nm in TEM pictures and the SAED (Selective Area Electron Diffraction) patterns in the inset. The lattice fringes between two adjacent planes are about 1 - 3 nm or less.

adjacent planes, about 1 - 3 nm in size or even less, in TEM images in **Figure 8**. These images show that the nanorods are composed of several hundred small zinc oxide NPs coated with green carboxylic fatty acid groups.

3.8.3. UV-Vis Absorption Spectroscopy Behavior of the Fine (1 - 3 nm) ZnO Q-Dot NPs in Nanofluid Formulation Product

Ultraviolet–visible absorption or ultraviolet–visible spectrophotometry (Varian, Australia) refers to the absorption of a light beam after passing through a sample (metallic NPs) or reflection from a sample surface. The UV-Vis spectral range is approximately 190 to 900 nm at room temperature. In nanotechnology science, according to the laws of quantum mechanics (quantum confinement), there is a clear relationship between the absorption wavelength and the diameter and size of NPs. As long as NPs absorb UV light at short wavelengths, they must be small (size-dependent emission). Usually, quantum dots are small semi-conducting NPs, and they thus absorb light in the ultraviolet wavelength range (depending on the size). Smaller Q-Dot NPs emit shorter wavelengths in the blue or green range (blue-shift or green-shift). Therefore, they show unique optical properties [14] [17]. On the other hand, the band gap of semiconductor NPs (SNP) can be changed with size, making them well-suited for biological applications. Therefore, the effective direct high band gap energy of Q-Dot NPs increases with decreasing the mean particle size, which means that the absorption edges spectrum blue-shifts with decreasing particle size (Brus' model) [55] [56] [57]. In fact, defect structures, oxygen vacancies (oxygen-deficient region and trapping states), production of oxygen radicals (reactive oxygen species (ROS), reactive surface sites and electron-hole pairs are crucial factors in the mechanism of ZnO Q-Dot NPs applications in the biomedical fields [14]. In ZnO NPs, a large number of valence-band (h^+) and/or conduction-band (e^-) are present even in the absence of UV-light because of the crystal defects of nanosized materials. In **Figure 9**, the UV-Vis (Perkin Elmer model lambda 35) absorption spectrum of ZnO Q-Dot NPs is shown and the maximum wavelength of zinc oxide Q-Dot NPs alone is 193 nm. This wavelength shifts to 194.3 in the nanodrug formulation. However, both wavelengths indicate that the NP is small in size. Actually, there are different extrinsic defect centers related to blue emissions and short wavelengths in UV-Vis spectroscopy. Herein, we can observe the multi-trapping states for ZnO Q-Dot NPs in spectrum b.

It is an interesting point that, regarding the remarkable synthesis of these ZnO NPs and their usage in nanoformulation to treat breast cancer, its high optical band gap energy was measured as 4.8 eV (for ZnO Q-Dot NPs alone) and 5.32 eV (for ZnO Q-Dot NPs in nanodrug formulation), respectively, which was much higher than that of the bulk type. In addition, positive zeta-potential (ζ) for ZnO Q-Dots NPs measured as the electric charge of these NPs in the water phase was +50 mV which indicates their complete dissolution and dispersion in water [14]. Cancerous cells are known to be comprised of a high concentration of anionic phospholipid (phosphatidylserine) on their outer membranes and

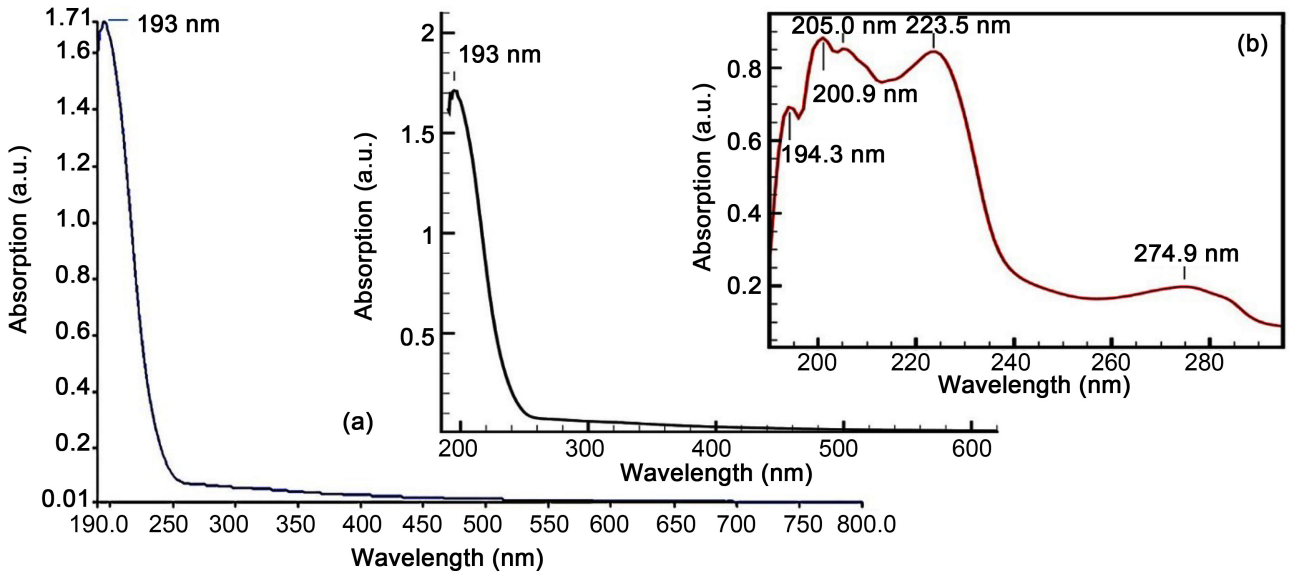

Figure 9. Spectroscopic curves of UV-Vis absorption of zinc oxide NPs and blue-shifted absorption edge. (a) ZnO Q-Dot NPs alone, and (b) ZnO Q-Dot NPs in the nanofluid formulation (nanodrug).

have large negative membrane potentials such that they can react chemically very quickly *via* electrostatic interactions. In addition to that, the unique electrostatic characteristics of ZnO NPs are another useful feature for their biomedical applications. The zinc oxide NPs typically have neutral hydroxyl groups (−OH) attached to their surface, which plays a significant role in their surface charge behavior. Such −OH groups are able to make the ZnO^{-} at high pHs and can produce $ZnOH_2^{+}$ in an aqueous medium at lower pHs. That is why zinc oxide NPs can create powerful electrical attractions with the surrounding environment of cancer cells in an aqueous environment (ROS generation). Accordingly, ZnO NPs can diffuse into the bacteria cell-wall and form great attraction and absorption forces between the opposite charges through intense electrostatic interaction and electrovalence bonding [58]. Of course, all these successful processes depend on the type of NP surface modifiers and the choice of new synthesis methods in nanotechnology science. The selection of NP surface modifiers and their functional groups play a major role in adsorption, surface tension, binding to the cancer cells, and activating NP surfaces. Therefore, the remarkable surface modifications of ZnO NPs have been used to further develop their stability and increase their selectivity to specific cells.

3.8.4. FTIR Spectroscopy of ZnO Q-Dot NPs Functionalized with Green Carbocyclic Acid

The functional groups of NPs in nanodrug formulation product were characterized by Fourier transform infrared (FTIR) spectroscopy using a Bruker Tensor 27, Billerica, MA-FTIR spectrophotometer in the range between 400 and 4000 cm^{-1} in KBr matrix. **Figure 10** shows the FTIR spectrum of the surface-modified ZnO NPs with green carboxylic fatty acid (C_{18}-COOH) and non-ionic ethoxylated surfactant in the polar solvent at pH = 9 - 11. The band at 555 cm^{-1} and

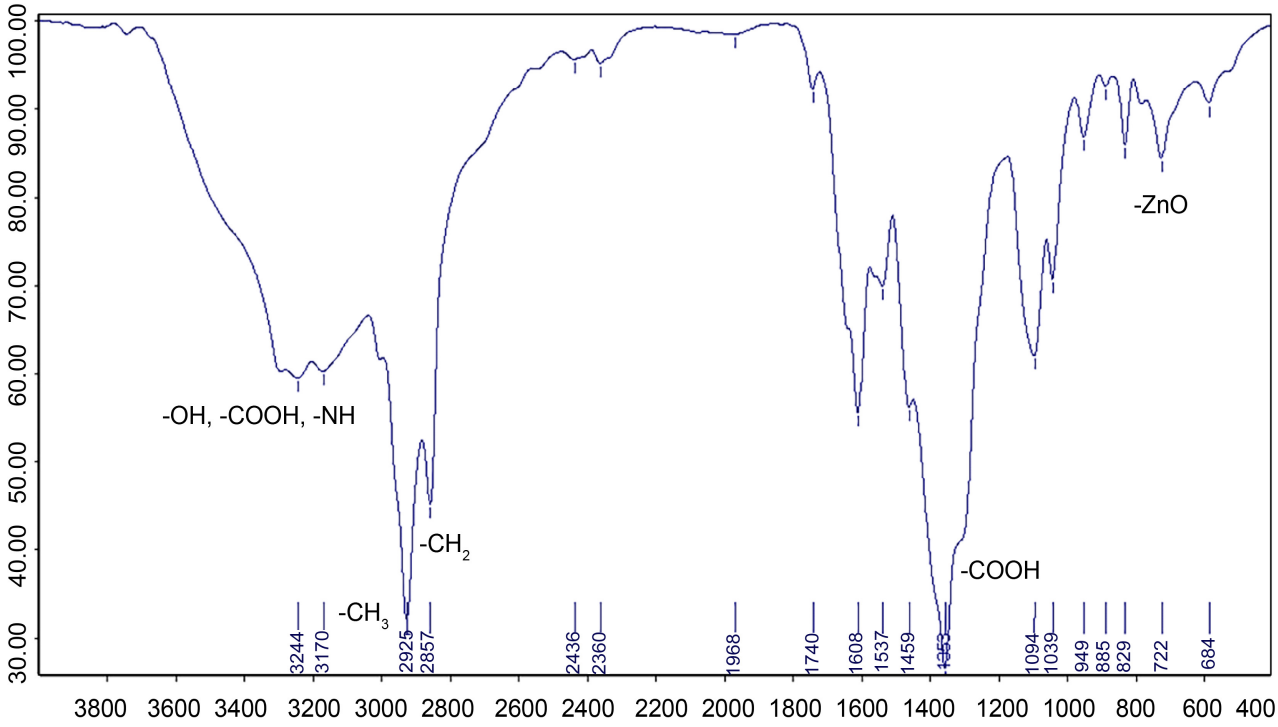

Figure 10. Fourier Transform Infrared (FTIR) spectrum of the hexagonal wurtzite structure of ZnO Q-Dot NPs with the space group P63mc, which were immersed in green carboxylic fatty acids (C18-COOH).

symmetric strong absorption vibration of –COOH and zinc carboxylate (COO–) groups at 1353 cm^{-1} correspond to the hexagonal Wurtzite structure of Zn-O. The broad and sharp stretching vibration mode of water's –OH band indicates the presence of a small amount of water adsorbed on the ZnO nanocrystal surface. The peaks corresponding to carbocyclic acid, –NH, and –C-H groups are observed in the range of 3244 - 2857 cm^{-1}. The lattice Zn-H_O bond in the defect structure of ZnO NPs is observed at 829 cm^{-1}, which is related to the substitutional hydrogen at the oxygen site (H_O), bounded to the lattice Zn site [59].

3.9. Biological Properties of ZnO Q-Dot Nanofluid Formulation Product (Nanodrug) as a Potent *in Vivo* Breast Cancer Treatment in Animal Model

Research Results Related to Our Theory

Many theories have been presented forward by biologists, professors of genetics, and chemists regarding the mechanism of action, production and growth of cancer cells in the human body. This section will address this issue from the nano-chemical aspect. The nanopharmaceuticals formulation should have specific NPs with a good tensile force on the cancerous glands (with their abnormal environmental characteristics). In this case, they can be absorbed by tumors, penetrate the cell membrane, and produce strong hydrogen bonds with the polar amino acids of the protein. Herein, the energetic NPs have more responsibility and can enter the membrane and move intelligently towards cancer cells without harming normal cells (according to animal model procedure results). Basically,

certain fluids are produced around cancer cells which is unusual, and this is an excellent signal for smart NPs to be absorbed into an uncommon environment. Another important point to note is that some cancers are produced by viruses with a sheath and a protein coating. In this process, the virus can break cystine covalent disulfide bonds (-S-S-) to two cysteine residues (HS-, thiol groups) and disrupt vital protein chains in the body, which is an important factor in the destruction of the biological systems of the body. Only cysteine and methionine contain a sulfur atom in their structures among the protein amino acids. In protein molecules, two cysteine residues often make a disulfide bond, which is essential in folding the proteins and stabilizing their structure. From the perspective of basic chemistry, this phenomenon is a dual redox reaction, which can occur between strong, suitable NPs and viruses, where the vital proteins of the body exist [60]. The virus has the power to exchange electrons, and when it enters the body, it can rupture important disulfide bonds through a reduction reaction, and produce two thiol anion bonds or their free radicals. Therefore, the human immune system would be weakened and disrupted. The stronger the virus, the more mutations it makes, during which time it can nest and spread itself. Thus, the cancer cells increase, gradually spread to all body parts and metastasize. The role of strong synthetic NPs with their special properties (like Q-Dot NPs) is significant and exciting at this stage. They must be able to both regenerate broken phosphorus and sulfur (disulfide bonds) containing compounds, such as DNA backbone and regulating enzymes (through the chemical oxidation reaction), and prevent the spread of causative viruses (through the reduction reaction) [60]. Surface trapping states, effective nanoporous and modified surface defects are the best essential characteristics of these Q-Dot NPs for pharmaceutical and nanomedicine industries. The destruction of tumor cells by Q-Dot NPs would probably happen selectively, which should be proved soon. Of course, the presence of useful surfactants (emulsion and stabilizing agent) in synthesizing these intelligently NPs, smart and accurate formulation of such biomedical nanomedicines are very significant and key strategies. Another common theory from a chemical point of view is the production of free radicals and various oxygen anions caused by the semi-conductivity of zinc oxide NPs, which is due to electron defects in their structure (resulting from reactive oxygen species ROS). This may affect some cellular components to induce the collapse of the membrane, resulting in cell decomposition and eventually death [61]. Intracellular ROS typically includes the superoxide radical anions ($O_2^{\bullet -}$), which in turn react with proton (H^+) to generate radicals ($HO_2^{\bullet}$) and finally hydrogen peroxide (H_2O_2), and hydroxyl radical ($^{\bullet}OH$), causing damage to cellular components such as lipids, DNA, mitochondrial damage followed by a loss in the balance of protein activities and ultimately leading to cancer cell apoptosis and cell death [48] [62] [63]. Scientists believe that endogenous hydrogen peroxide (H_2O_2 as a cancer diagnostic marker) is a toxic compound made by photodynamic therapy (PDT) which can induce cell death in cancer patients and act as

stimulation of anti-tumor immune response (due to oxidative stress, cell killing, necrotic cell death and apoptosis death of the tumor cells) [64] [65]. On the other hand, with the expansion of various novel nanomaterials, photodynamic therapy (PDT) employs a light-excited photosensitizer (PS) to generate reactive oxygen species (ROS) in the presence of oxygen (O_2), which leads to the destruction of mitochondria and eventually cell death. Interestingly, the conduction band's electrons are good reducers in crystal defects of ZnO NPs, which can lead to a large number of electron-hole pairs ($e^- - h^+$). These holes (or unoccupied states in the valence band) are powerful oxidizing agents in ZnO NPs and can split water molecules derived from the ZnO aqueous environment into H^+ and OH^- [66]. The significant property of photoactivation in semiconductors materials such as quantum dots (Q-Dots) and ZnO NPs can lead to the further secretion of ROS. Effectively targeting the cancer cells would lead to their selective destruction. Moreover, owing to the wide uses of novel zinc oxide Q-Dot NPs in all aspects of life, such as toxicological research (especially antibacterial, antifungal, antiviral, and anticancer qualities in therapeutic intervention and drug delivery), they have recently received increasing attention [67]. In fact, Q-Dot NPs can react with H_2O_2 and H^+ in the tumor microenvironment (TME) to generate oxygen (O_2) and overcome tumor hypoxia, just like an oxygen-generation nano-factory (chemical oxidation reaction) [68].

3.10. Pursuing the Efficacy of ZnO Q-Dot NPs in Targeted Tumor Treatment by Photoluminescence (PL) Spectra

The fine zinc oxide Q-Dot NPs in this combined formulation is primarily responsible for attacking the skin membranes of breast cancer cells since they have great oxygen vacancy and high diffusion coefficients, particularly at elevated temperatures [66]. These fine NPs have very high energy levels in hydrophilic nanofluids and can penetrate cancer cell lines through the formation and production of very strong and stable hydrogen bonds (as the first chemical reaction) in contact with the amino acids present in cell membrane proteins during nanodrug therapy. The greater these connections to the skin membrane, the greater the penetration of the nanodrug into the cells until the cell breaks down and dies. In this nanodrug formulation, the presence of ZnO@PVP nanopolymer was used to aid ZnO Q-Dot NPs in aqueous solutions. In fact, polymer nanocomposites play an excellent role in increasing the activity and production of hydrogen bonds and show a synergistic effect in the transfer of electrons and great conductivity through electrostatic attractions. As the size of Q-Dot NPs becomes smaller, photon absorption occurs at higher energies. Thus, in the ultraviolet absorption spectrum of the product, some peaks are observed in short wavelengths. The optical properties of very fine NPs are more prominent in semiconductors. These nanomaterials' optical properties are directly related to the type of electronic structure of NPs and their size, so that the intensity of the optical spectrum of the semi-conducting NPs changes with their size. In general, the

transfer of light spectrum to higher energies due to NP size reduction means an increase in the band gap energy and the number of electron-hole pairs. Because of this process, the band gap energy has been calculated to be 5.32 electron volts for this formulated nanodrug. In fact, the presence of free electrons in the structure of NPs causes more energy to be produced on their surface, making them more active and daring in destroying cancerous tumors. Here, it is worth noting that the photoluminescence spectra in Figure 11 show the UV light emission of ZnO Q-Dot NPs. This Figure illustrates the various radiation curves (photoluminescence intensity in terms of wavelength) at exciting wavelengths 227, 259, 280, 330, and 370 nm in the blue shift area, where various structural electron defects exist can be observed as a broad curve. This trend indicates the presence of surface energy transitions due to lattice structural morphologies and defects, surface functionalization, surface oxygen vacancies (mobile ionic defects), and trapping states in Q-Dot NPs. As mentioned, the electrons left over from oxygen vacancies increase the Q-Dot NP's surface activity due to the enhancement of the surface area and the quantum confinement effect ("particle-in-a-box"). This event is considered when the electron wave-function is influenced by the small size of the NPs, blue shift absorbance, and excellent fluorescence [54] [69]. Many studies have shown that the cytotoxic properties of ZnO NPs and their strong nanocomposites (when ZnO NPs act as vigorous activators over a substrate) against various cancerous cells are directly related to size and dose-response

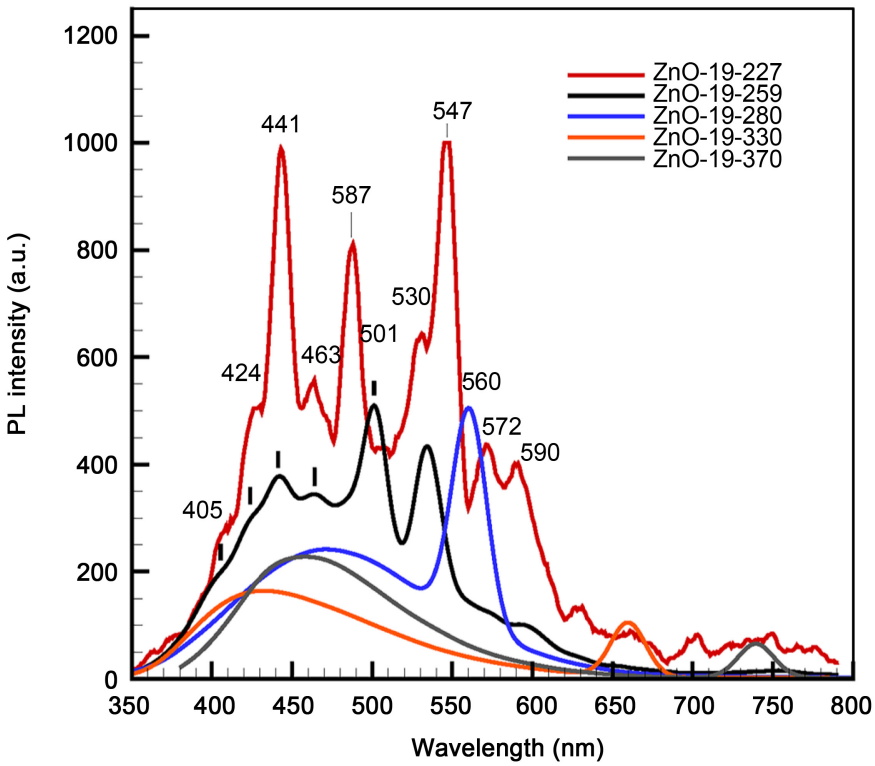

Figure 11. Photoluminescence (PL) emission spectra of the ZnO Q-Dot NPs at different visible emission wavelengths in the range of λ = 227, 259, 280, 330, and 370 nm.

correlation between concentration and cellular viability, whereas smaller NPs are showing greater toxicity. Because there are more pores on the high surface area naturally, more reactions occur on the surface [70] [71]. Due to the inherent photoluminescence properties, which can be useful in biosensing applications, recent studies have reported that ZnO nanomaterials and nanocomposites are considered promising and make them a suitable choice for anticancer medicines.

The visible emission peaks blue-shift to the positions with shorter wavelengths which can be ascribed to quantum size effects (size-dependent behaviors). The synthesized ZnO Q-Dot NPs exhibited a broad band and a strong visible emission peak centered in the 300 - 350 nm range, including a few short, long, and wide trapping states in its quantum transition states.

4. Conclusion

This is very interesting, accurate, practical and academic research performed in collaboration with nanomedicine experts for over three years. In this research, a novel nanomedicine was formulated using zinc oxide Q-Dot NPs as the main component and zinc oxide nanopolymer solution as the coherent and adjuvant along with various wetting agents, dispersants, suitable emulsifiers and binding agent polymers in eco-friendly polar solvent/water mixtures in the nanoformulation. Notably, this nanofluid/nanodrug is very stable in aqueous solutions and does not decompose at the pH of nanofluid. This nanodrug was used to treat mice (BALB/c) with serious breast cancer, which had become cancerous by the 4T1 cell line (we invite the readers to also see the supplementary figures of laboratory animal models attached to this paper). The nanodrug is delivered through various methods, especially in the form of mandatory and optional oral administration using a 40 μg/ml dose during treatment for two weeks. Notably, the use of this nanodrug through various injection methods (intravenous IVP (injection into a mouse tail vein) and abdominal cavity) and the diversity of oral methods worked very well. No traces of cancerous glands were observed in the pathology, nor was there any metastasis. According to the pathology results, all cancerous glands had disappeared (100%). These findings provide a new perspective on the use of modern nanomedicines in treating breast cancer without chemotherapy and stress. NPs activate the induction pathway of apoptosis, releasing the cytochrome C, increasing the expression of the caspase-3 protease gene in cancer cells, and inducing programmed cell death (apoptosis). Herein, the choice of NPs such as healthy zinc oxide Q-Dot NPs and the selection of effective auxiliary major components in the formulation of nanodrug also play critical roles in the success of this nanoproduct. They are not toxic at all and deliver the best efficiency with the lowest amount. The key point is that the mice treated with the nanodrug were kept in standard laboratory conditions for nine months, and in the end, they showed no signs of metastasis, spread tumors, or side effects. The recovered mice regained their health, continued their eating habits, and even had a safe space to mate. Interestingly, none of the children in

this generation of mice were sick and no signs of cancerous tumors and metastases were observed in their tissues and organs after 9 months (this was a valuable achievement and our gold standard). This novel nanodrug could be very effective for the clinical treatment of volunteer breast cancer patients.

Acknowledgements

The authors are honored to thank the Nanomedicine & Nanodrugs ZPH company team for their authentic knowledge of NPs and the unique properties of Q-Dot NPs in nanoformulations. Further, special thanks to Professor Azizollah Shafiekhani from Alzahra University, an outstanding physicist, for extraordinary suggestions on new UV-Vis, photoluminescence, and band gap energy physics topics. Moreover, sincere gratitude to Mrs. Marjan Chaiatri, a graphic designer from Florida Atlantic University, for the graphical supports. The team of authors would also like to thank Mr. Engineer Hamid Rahdar for his extensive and up-to-date studies on the mechanism of cancer.

Conflicts of Interest

The authors declare that the research was conducted without any commercial or financial relationships, which could be construed as a potential conflict of interest. In addition, the authors declare no potential conflicts of interest and are responsible for the content and writing of the manuscript.

References

[1] Hajj, M.A., Wicha, M.S., Hernandez, A.B., Morrison, S.J. and Clarke, M.F. (2003) Prospective Identification of Tumorigenic Breast Cancer Cells. *Proceedings of the National Academy of Sciences of the United States of America*, **100**, 3983-3988. https://doi.org/10.1073/pnas.0530291100

[2] Spellman, P. and Gray, J. (2011) A New Treasure in the Breast Cancer Gene Hunt. *Nature Medicine*, **17**, 422-423. https://doi.org/10.1038/nm0411-422

[3] Feng, Y., Spezia, M., Huang, S., Yuan, C., Zeng, Z., Zhang, L., Ji, X., Liu, W., Huang, B., Luo, W., Liu, B., Lei, Y., Du, S., Vuppalapati, A., Luu, H.H., Haydon, R.C., He, T.C. and Ren, G. (2018) Breast Cancer Development and Progression: Risk Factors, Cancer Stem Cells, Signaling Pathways, Genomics, and Molecular Pathogenesis. *Genes & Diseases*, **5**, 77-106. https://doi.org/10.1016/j.gendis.2018.05.001

[4] Valko, M., Rhodes, C.J., Moncol, J., Izakovic, M. and Mazur, M. (2006) Free Radicals, Metals and Antioxidants in Oxidative Stress-Induced Cancer. *Chemico-Biological Interactions*, **160**, 1-40. https://doi.org/10.1016/j.cbi.2005.12.009

[5] Sies, H. (1997) Oxidative Stress: Oxidants and Antioxidants. *Experimental Physiology*, **82**, 291-295. https://doi.org/10.1113/expphysiol.1997.sp004024

[6] Kohen, R. and Nyska, A. (2002) Invited Review: Oxidation of Biological Systems: Oxidative Stress Phenomena, Antioxidants, Redox Reactions, and Methods for Their Quantification. *Toxicologic Pathology*, **30**, 620-650. https://doi.org/10.1080/01926230290166724

[7] Khanna, P., Ong, C., Bay, B. and Baeg, G. (2015) Nanotoxicity: An Interplay of Oxidative Stress, Inflammation and Cell Death. *Nanomaterials* (*Basel*), **5**, 1163-1180. https://doi.org/10.3390/nano5031163

[8] Fakhroueian, Z., Mozafari Dehshiri, A., Katouzian, F. and Esmaeilzadeh, P. (2014) *In Vitro* Cytotoxic Effects of Modified Zinc Oxide Quantum Dots on Breast Cancer Cell Lines (MCF7), Colon Cancer Cell Lines (HT29) and Various Fungi. *Journal of Nanoparticle Research*, **16**, 2483. https://doi.org/10.1007/s11051-014-2483-2

[9] Ali, A., Phull, A.R. and Zia, M. (2018) Elemental Zinc to Zinc Nanoparticles: Is ZnO NPs Crucial for Life? Synthesis, Toxicological, and Environmental Concerns. *Nanotechnology Reviews*, **7**, 413-441. https://doi.org/10.1515/ntrev-2018-0067

[10] Wiesmann, N., Tremel, W. and Brieger, J. (2020) Zinc Oxide Nanoparticles for Therapeutic Purposes in Cancer Medicine. *Journal of Materials Chemistry B*, **8**, 4973-4989. https://doi.org/10.1039/D0TB00739K

[11] Martirosyan, A. and Schneider, Y.J. (2014) Engineered Nanomaterials in Food: Implications for Food Safety and Consumer Health. *International Journal of Environmental Research and Public Health*, **11**, 5720-5750. https://doi.org/10.3390/ijerph110605720

[12] Sachdeva, H. and Saroj, R. (2013) ZnO Nanoparticles as an Efficient, Heterogeneous, Reusable, and Ecofriendly Catalyst for Four-Component One-Pot Green Synthesis of Pyranopyrazole Derivatives in Water. *The Scientific World Journal*, **2013**, Article ID: 680671. https://doi.org/10.1155/2013/680671

[13] Sun, Y., Chen, L., Bao, Y., Zhang, Y., Wang, J., Fu, M., Wu, J. and Ye, D. (2016) The Applications of Morphology Controlled ZnO in Catalysis. *Catalysts*, **6**, Article No. 188. https://doi.org/10.3390/catal6120188

[14] Fakhroueian, Z., Vahabpour, R., Assmar, M., Massiha, A., Zahedi, A., Esmaeilzadeh, P., Katouzian, F., Rezaei, S., Keyhanvar, P. and Mozafari Dehshiri, A. (2018) ZnO Q-Dots as a Potent Therapeutic Nanomedicine for *in Vitro* Cytotoxicity Evaluation of Mouth KB44, Breast MCF7, Colon HT29 and HeLa Cancer Cell Lines, Mouse Ear Swelling Tests *in Vivo* and Its Side Effects Using the Animal Model. *Artificial Cells, Nanomedicine, and Biotechnology*, **46**, 96-111. https://doi.org/10.1080/21691401.2018.1452023

[15] Rahman, W., Garain, S., Sultana, A., Middya, T.R. and Mandal, D. (2018) Self-Powered Piezoelectric Nanogenerator Based on Wurtzite ZnO Nanoparticles for Energy Harvesting Application. *Materials Today: Proceedings*, **5**, 9826-9830. https://doi.org/10.1016/j.matpr.2017.10.173

[16] Dayem, A.A., Hossain, M.K., Lee, S.B., Kim, K., Saha, S.K., Yang, G.M., Choi, H.Y. and Cho, S.G. (2017) The Role of Reactive Oxygen Species (ROS) in the Biological Activities of Metallic Nanoparticles. *International Journal of Molecular Sciences*, **18**, Article No. 120. https://doi.org/10.3390/ijms18010120

[17] Fakhroueian, Z., Katouzian, F., Esmaeilzadeh, P., Moradi Bidhendi, S. and Esmaeilzadeh, P. (2019) Enhanced Engineered ZnO Nanostructures and Their Antibacterial Activity against Urinary, Gastrointestinal, Respiratory and Dermal Genital Infections. *Applied Nanoscience*, **9**, 1759-1773. https://doi.org/10.1007/s13204-019-00996-5

[18] Guerrini, L., Alvarez-Puebla, R.A. and Pazos-Perez, N. (2018) Surface Modifications of Nanoparticles for Stability in Biological Fluids. *Materials*, **11**, Article No. 1154. https://doi.org/10.3390/ma11071154

[19] Batool, M., Khurshid, S., Daoush, W.M., Siddique, S.A. and Nadeem, T. (2021) Green Synthesis and Biomedical Applications of ZnO Nanoparticles: Role of PEGylated-ZnO Nanoparticles as Doxorubicin Drug Carrier against MDA-MB-231(TNBC) Cells Line. *Crystals*, **11**, 344. https://doi.org/10.3390/cryst11040344

[20] Chang, Y.N., Zhang, M., Xia, L., Zhang, J. and Xing, G. (2012) The Toxic Effects

and Mechanisms of CuO and ZnO Nanoparticles. *Materials*, **5**, 2850-2871. https://doi.org/10.3390/ma5122850

[21] Chen, Z., Tian, R., She, Z., Cai, J. and Li, H. (2020) Role of Oxidative Stress in the Pathogenesis of Nonalcoholic Fatty Liver Disease. *Free Radical Biology and Medicine*, **152**, 116-141. https://doi.org/10.1016/j.freeradbiomed.2020.02.025

[22] Siddiqi, K.S., Rahman, A.U., Uddin, T. and Husen, A. (2018) Properties of Zinc Oxide Nanoparticles and Their Activity against Microbes. *Nanoscale Research Letters*, **13**, Article No. 141. https://doi.org/10.1186/s11671-018-2532-3

[23] Khan, I., Saeed, K. and Khan, I. (2019) Nanoparticles: Properties, Applications and Toxicities. *Arabian Journal of Chemistry*, **12**, 908-931. https://doi.org/10.1016/j.arabjc.2017.05.011

[24] Manke, A., Wang, L. and Rojanasakul, Y. (2013) Mechanisms of Nanoparticle-Induced Oxidative Stress and Toxicity. *BioMed Research International*, **2013**, Article ID: 942916. https://doi.org/10.1155/2013/942916

[25] Jonkers, J. and Derksen, P.W. (2007) Modeling Metastatic Breast Cancer in Mice. *Journal of Mammary Gland Biology and Neoplasia*, **12**, 191-203. https://doi.org/10.1007/s10911-007-9050-8

[26] Xanthopoulos, J.M., Romano, A. and Majumdar, S.K. (2005) Response of Mouse Breast Cancer Cells to Anastrozole, Tamoxifen, and the Combination. *Journal of Biomedicine and Biotechnology*, **2005**, 10-19. https://doi.org/10.1155/JBB.2005.10

[27] Pulaski, B.A. and Ostrand-Rosenberg, S. (2001) Mouse 4T1 Breast Tumor Model. In: *Current Protocols in Immunology*, John Wiley, New York, Chapter 20, Unit 20.2.

[28] DuPre, S.A., Redelman, D. and Hunter, K.W. (2007) The Mouse Mammary Carcinoma 4T1: Characterization of the Cellular Landscape of Primary Tumors and Metastatic Tumor Foci. *International Journal of Experimental Pathology*, **88**, 351-360. https://doi.org/10.1111/j.1365-2613.2007.00539.x

[29] Baliga, M.S., Meleth, S. and Katiyar, S.K. (2005) Growth Inhibitory and Antimetastatic Effect of Green Tea Polyphenols on Metastasis-Specific Mouse Mammary Carcinoma 4T1 Cells *in Vitro* and *in Vivo* Systems. *Clinical Cancer Research*, **11**, 1918-1927. https://doi.org/10.1158/1078-0432.CCR-04-1976

[30] Jones, L.W., Viglianti, B.L., Tashjian, J.A., Kothadia, S.M., Keir, S.T., Freedland, S.J., Potter, M.Q., Moon, E.J., Schroeder, T., Herndon, J.E. and Dewhirst, M.W. (2010) Effect of Aerobic Exercise on Tumor Physiology in an Animal Model of Human Breast Cancer. *Journal of Applied Physiology* (1985), **108**, 343-348. https://doi.org/10.1152/japplphysiol.00424.2009

[31] Foster, H.L., Small, J.D. and Fox, J.G. (1983) The Mouse in Biomedical Research. Vol. 3, Academic Press, New York, 402-437.

[32] Nemzek, J.A., Bolgos, G.L., Williams, B.A. and Remick, D. (2001) Differences in Normal Values for Murine White Blood Cell Counts and Other Hematological Parameters Based on Sampling Site. *Inflammation Research*, **50**, 523-527. https://doi.org/10.1007/PL00000229

[33] Klonz, A., Wonigeit, K., Pabst, R. and Westermann, J. (1996) The Marginal Blood Pool of the Rat Contains Not Only Granulocytes, But Also Lymphocytes, NK-Cells and Monocytes: A Second Intravascular Compartment, Its Cellular Composition, Adhesion Molecule Expression and Interaction with the Peripheral Blood Pool. *Scandinavian Journal of Immunology*, **44**, 461-469. https://doi.org/10.1046/j.1365-3083.1996.d01-334.x

[34] Nurhayati, A.P.D., Pratiwi, R. and Soekardiman (2019) Total and Differential Cells

of Leukocyte Mice (Musmusculus) on Evaluation *in Vivo* Anticancer Extracts Ethanol Marine Sponges *Aaptos suberitoides*. *Journal of Physics*: *Conference Series*, **1374**, Article ID: 012031. https://doi.org/10.1088/1742-6596/1374/1/012031

[35] Sun, D., Zhou, S. and Gao, W. (2020) What Went Wrong with Anticancer Nanomedicine Design and How to Make It Right. *ACS Nano*, **14**, 12281-12290. https://doi.org/10.1021/acsnano.9b09713

[36] Yelek, C., Mignion, L., Paquot, A., Bouzin, C., Corbet, C., Muccioli, G.G., Cani, P.D. and Jordan, B.F. (2022) Tumor Metabolism Is Affected by Obesity in Preclinical Models of Triple-Negative Breast Cancer. *Cancers*, **14**, 562.1-16. https://doi.org/10.3390/cancers14030562

[37] Ahmad, S., Idris, R.A.M., Hanaffi, W.N.W., Perumal, K., Boer, J.C., Plebanski, M., Jaafar, J., Lim, J.K. and Mohamud, R. (2020) Cancer Nanomedicine and Immune System—Interactions and Challenges. *Frontiers in Nanotechnology*, **3**, Article ID: 681305. https://doi.org/10.3389/fnano.2021.681305

[38] Yu, H.J. and Geest, B.G.D. (2020) Nanomedicine and Cancer Immunotherapy. *Acta Pharmacologica Sinica*, **41**, 879-880. https://doi.org/10.1038/s41401-020-0426-2

[39] Li, J. and Burgess, D.J. (2020) Nanomedicine-Based Drug Delivery towards Tumor Biological and Immunological Microenvironment. *Acta Pharmaceutica Sinica B*, **10**, 2110-2124. https://doi.org/10.1016/j.apsb.2020.05.008

[40] Wang, E.C. and Wang, A.Z. (2015) Nanoparticles and Their Applications and Molecular Biology. *Integrative Biology*, **6**, 9-26.

[41] Zhang, H., Song, F., Dong, C., Yu, L., Chang, C. and Chen, Y. (2021) Co-Delivery of Nanoparticle and Molecular Drug by Hollow Mesoporous Organosilica for Tumor-Activated and Photothermal-Augmented Chemotherapy of Breast Cancer. *Nanobiotechnology*, **19**, 290. https://doi.org/10.1186/s12951-021-01025-w

[42] Rosen, L.S., Ashurst, H.L. and Chap, L. (2010) Targeting Signal Transduction Pathways in Metastatic Breast Cancer: A Comprehensive Review. *Oncologist*, **15**, 216-235. https://doi.org/10.1634/theoncologist.2009-0145

[43] Weigelt, B., Baehner, F.L. and Reis-Filho, J.S. (2010) The Contribution of Gene Expression Profiling to Breast Cancer Classification, Prognostication and Prediction: A Retrospective of the Last Decade. *The Journal of Pathology*, **220**, 263-280. https://doi.org/10.1002/path.2648

[44] Aslakson, C.J. and Miller, F.R. (1992) Selective Events in the Metastatic Process Defined by Analysis of the Sequential Dissemination of Subpopulations of a Mouse Mammary Tumor. *Cancer Research*, **52**, 1399-1405.

[45] Steenbrugge, J., Elst, N.V., Demeyere, K., Wever, O.D., Sanders, N.N., Broeck, W.V.D., Dirix, L., Laere, S.V. and Meyer, E. (2019) Comparative Profiling of Metastatic 4T1- vs. Non-Metastatic Py230-Based Mammary Tumors in an Intraductal Model for Triple-Negative Breast Cancer. *Frontiers in Immunology*, **10**, Article No. 2928. https://doi.org/10.3389/fimmu.2019.02928

[46] Salmon, P. and Trono, D. (2006) Chapter 4. Production and Titration of Lentiviral Vectors. In: *Current Protocols in Neuroscience*, Wiley, Hoboken, Unit 4.21. https://doi.org/10.1002/0471142301.ns0421s37

[47] Gumireddy, K., Sun, F., Klein-Szanto, A.J., Gibbins, J.M., Gimotty, P.A., Saunders, A.J., Schultz, P.G. and Huang, Q. (2007) *In Vivo* Selection for Metastasis Promoting Genes in the Mouse. *Proceedings of the National Academy of Sciences of the United States of America*, **104**, 6696-6701. https://doi.org/10.1073/pnas.0701145104

[48] Anjum, S., Hashim, M., Malik, S.A., Khan, M., Lorenzo, J.M., Abbasi, B.H. and Hano, C. (2021) Recent Advances in Zinc Oxide Nanoparticles (ZnO NPs) for Cancer

Diagnosis, Target Drug Delivery, and Treatment. *Cancers*, **13**, Article No. 4570. https://doi.org/10.3390/cancers13184570

[49] Aalami, A.H., Mesgari, M. and Sahebkar, A. (2020) Synthesis and Characterization of Green Zinc Oxide Nanoparticles with Antiproliferative Effects through Apoptosis Induction and MicroRNA Modulation in Breast Cancer Cells. *Bioinorganic Chemistry and Applications*, **2020**, Article ID: 8817110. https://doi.org/10.1155/2020/8817110

[50] Mercogliano, M.F., Bruni, S., Elizalde, P.V. and Schillaci, R. (2020) Tumor Necrosis Factor α Blockade: An Opportunity to Tackle Breast Cancer. *Frontiers in Oncology*, **10**, Article No. 584. https://doi.org/10.3389/fonc.2020.00584

[51] Bertazza, L. and Mocellin, S. (2010) The Dual Role of Tumor Necrosis Factor (TNF) in Cancer. *Biology*, **17**, 3337-3352. https://doi.org/10.2174/092986710793176339

[52] Moussodia, R.O., Balan, L., Merlin, C., Mustin, C. and Schneider, R. (2010) Biocompatible and Stable ZnO Quantum Dots Generated by Functionalization with Siloxane-Core PAMAM Dendrons. *Journal of Materials Chemistry*, **20**, 1147-1155. https://doi.org/10.1039/B917629B

[53] Schneider, R., Balan, L. and Aldeek, F. (2011) Synthesis, Characterization and Biological Applications of Water-Soluble ZnO Quantum Dots. In: Rahman, R., Ed., *Nanomaterials*, Intech, London, 27-42. https://doi.org/10.5772/27238

[54] Singh, P., Singh, R.K. and Kumar, R. (2021) Journey of ZnO Quantum Dots from Undoped to Rare-Earth and Transition Metal-Doped and Their Applications. *RSC Advances*, 11, 2512-2545. https://doi.org/10.1039/D0RA08670C

[55] Pesika, N.S., Stebe, K.J. and Searson, P.C. (2003) Relationship between Absorbance Spectra and Particle Size Distributions for Quantum-Sized Nanocrystals. *The Journal of Physical Chemistry B*, **107**, 10412-10415. https://doi.org/10.1021/jp0303218

[56] Viswanatha, R., Sapra, S., Satpati, B., Satyam, P.V., Dev, B.N. and Sarma, D.D. (2004) Understanding the Quantum Size Effects in ZnO Nanocrystals. *Journal of Materials Chemistry*, **14**, 661-668. https://doi.org/10.1039/b310404d

[57] Yousefi, A.M., Safaroghli-Azar, A., Fakhroueian, Z. and Bashash, D. (2020) ZnO/CNT@Fe_3O_4 Induces ROS-Mediated Apoptosis in Chronic Myeloid Leukemia (CML) Cells: An Emerging Prospective for Nanoparticles in Leukemia Treatment. *Artificial Cells, Nanomedicine, and Biotechnology*, **48**, 735-745. https://doi.org/10.1080/21691401.2020.1748885

[58] Chen, T., Zhao, T., Wei, D., Wei, Y., Li, Y. and Zhang, H. (2013) Core-Shell Nanocarriers with ZnO Quantum Dots-Conjugated Au Nanoparticle for Tumor-Targeted Drug Delivery. *Carbohydrate Polymers*, **92**, 1124-1132. https://doi.org/10.1016/j.carbpol.2012.10.022

[59] Kumari, R., Sahai, A. and Goswami, N. (2015) Effect of Nitrogen Doping on Structural and Optical Properties of ZnO Nanoparticles. *The Journal of Progress in Natural Science: Materials International*, **25**, 300-309. https://doi.org/10.1016/j.pnsc.2015.08.003

[60] Fakhroueian, Z., Esmaeilzadeh, P. and Esmaeilzadeh, P. (2020) The Mirror Strategy of Nanoparticles against the Coronavirus. *International Journal of Nanotechnology in Medicine & Engineering*, **5**, 1-4. https://doi.org/10.20944/preprints202007.0443.v1

[61] Liao, C., Jin, Y., Li, Y. and Tjong, S.C. (2020) Interactions of Zinc Oxide Nanostructures with Mammalian Cells: Cytotoxicity and Photocatalytic Toxicity. *International Journal of Molecular Sciences*, **21**, 6305. https://doi.org/10.3390/ijms21176305

[62] Ostrovsky, S., Kazimirsky, G., Gedanken, A. and Brodie, C. (2009) Selective Cytotoxic Effect of ZnO Nanoparticles on Glioma Cells. *Nano Research*, **2**, 882-890. https://doi.org/10.1007/s12274-009-9089-5

[63] Nair, S., Sasidharan, A., Rani, V.V.D., Menon, D., Nair, S., Manzoor, K. and Raina, S. (2009) Role of Size Scale of ZnO Nanoparticles and Microparticles on Toxicity toward Bacteria and Osteoblast Cancer Cells. *Journal of Materials Science*: *Materials in Medicine*, **20**, S235-S241. https://doi.org/10.1007/s10856-008-3548-5

[64] Zhang, Y., Zhang, J., Jia, Q., Ge, J. and Wang, P. (2021) Innovative Strategies of Hydrogen Peroxide-Involving Tumor Therapeutics. *Materials Chemistry Frontiers*, **5**, 4474-4501. https://doi.org/10.1039/D1QM00134E

[65] Ameisen, J.C. (2002) On the Origin, Evolution, and Nature of Programmed Cell Death: A Timeline of Four Billion Years. *Cell Death and Differentiation*, **9**, 367-393. https://doi.org/10.1038/sj.cdd.4400950

[66] Rasmussen, J.W., Martinez, E., Louka, P. and Wingett, D.G. (2010) Zinc Oxide Nanoparticles for Selective Destruction of Tumor Cells and Potential for Drug Delivery Applications. *Expert Opinion on Drug Delivery*, **7**, 1063-1077. https://doi.org/10.1517/17425247.2010.502560

[67] Wiesmann, N., Tremel, W. and Brieger, J. (2020) Zinc Oxide Nanoparticles for Therapeutic Purposes in Cancer Medicine. *Journal of Materials Chemistry B*, **23**, 4973-4989. https://doi.org/10.1039/D0TB00739K

[68] Thangudu, S. and Su, C.H. (2021) Peroxidase Mimetic Nanozymes in Cancer Phototherapy: Progress and Perspectives. *Biomolecules*, **11**, Article No. 1015. https://doi.org/10.3390/biom11071015

[69] Gunkel, F., Christensen, D.V., Chen, Y.Z. and Pryds, N. (2020) Oxygen Vacancies: The (In)visible Friend of Oxide Electronics. *Applied Physics Letters*, **116**, Article ID: 120505. https://doi.org/10.1063/1.5143309

[70] Scherzad, A., Meyer, T., Kleinsasser, N. and Hackenberg, S. (2017) Molecular Mechanisms of Zinc Oxide Nanoparticle-Induced Genotoxicity. *Materials*, **10**, Article No. 1427. https://doi.org/10.3390/ma10121427

[71] Yousefi, A.M., Azar, A.S., Sigaroodi, A.P., Fakhroueian, Z., Momeny, M. and Bashash, D. (2021) Application of ZnO/CNT@Fe_3O_4 Nanocomposite in Amplifying the Anti-Leukemic Effects of Imatinib: A Novel Strategy to Adjuvant Therapy in Chronic Myeloid Leukemia. *Biomedical Materials*, **16**, Article ID: 035029. https://doi.org/10.1088/1748-605X/abcae2

Supplementary Data

Images of extensive research on the effect of synthesized nanodrug on animal models:

Figure S1. The mice holding box (left) and the mouse in which a tumor lesion was observed (right).

Figure S2. Preparation of the animal under investigation for nanodrug injection.

Figure S3. Intraperitoneal injection (abdominal cavity) of synthesized nanodrug to the sensitive animal.

Figure S4. Evaluation of the therapeutic effect of orally administered synthesized nanodrug on animals in the study group, in which tissue changes were examined in terms of size and response power to nanodrug within two weeks of drug administration.

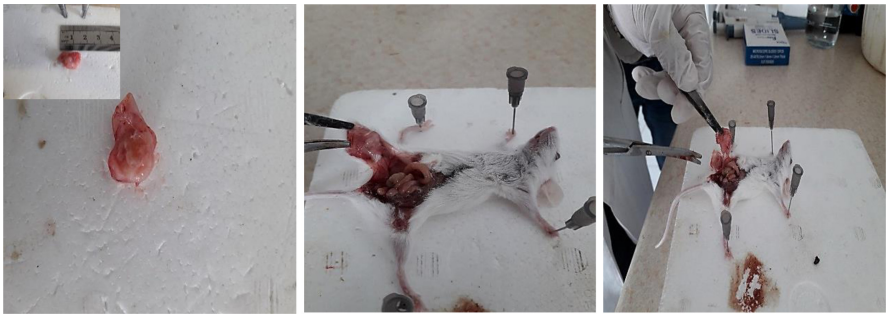

Figure S5. Extracting and measuring the cancerous gland, providing the role of reference control for this project.

Figure S6. Examination of the breast tissue of the examined animal after using the formulated nanodrug.

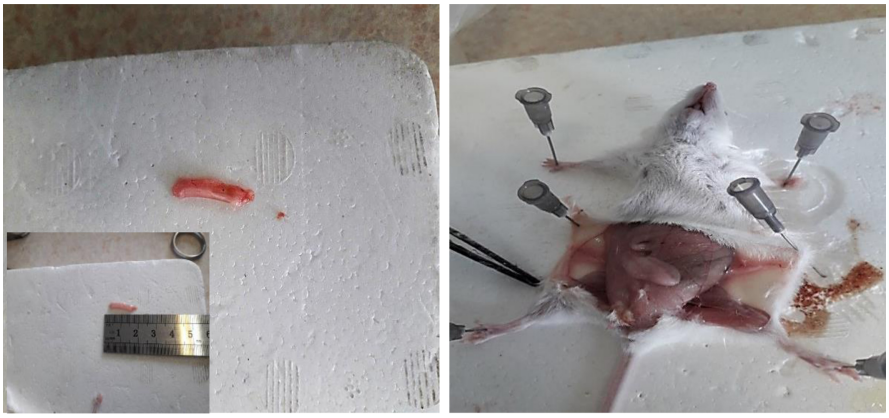

Figure S7. Consideration of tissue samples in a nanodrug-treated animal at a concentration of 40 μg/ml indicates improvement in breast tissues under nanodrug actions through oral therapy.

Figure S8. The process of taking blood from the ocular cavernoma to prepare a blood smear. Orbital tumors are abnormal tissue masses in structures around the eye. These lesions may be benign or malignant and originate in the eye's orbit or spread elsewhere in the body (metastasize).

Figure S9. Nanodrug-treated healthy mice, through intravenous injection (left) and oral administration (right), show their lively activities in their boxes. The vitality, health, movement and fast jumping of the treated mice, along with proper nutrition, are very promising after the optimal recovery.

Figure S10. Preparation of nanomedicine of the claimed product for injection into sensitive animals.

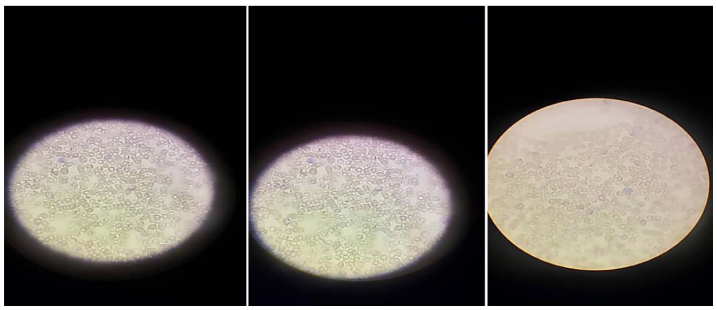

Figure 11. Investigating the blood spread of sensitive laboratory animals infected with the cancer cell line.

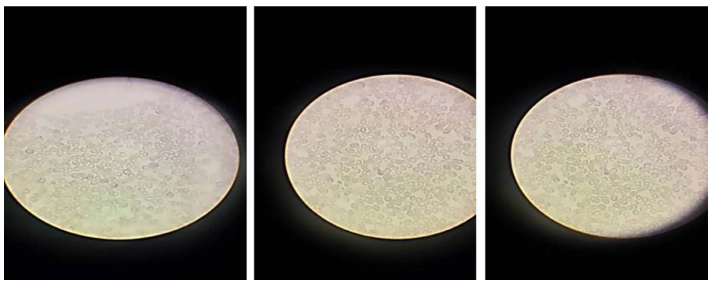

Figure S12. Morphological investigations of mice infected with cancer cell line via blood cell expansion under the microscope.

Figure S13. Taking out a breast cancer tissue sample in the control group animal and measuring the cancer tumor obtained from the disease.

Figure S14. Examining the tissue sample in an animal treated with nanomedicine with a concentration of 40 μg/ml shows improvement in the breast tissue. Herein, on the left side, the breast tissue obtained from the animal treated with nanomedicine by oral treatment method is seen (within two weeks after receiving nanomedicine without processing chemotherapy).

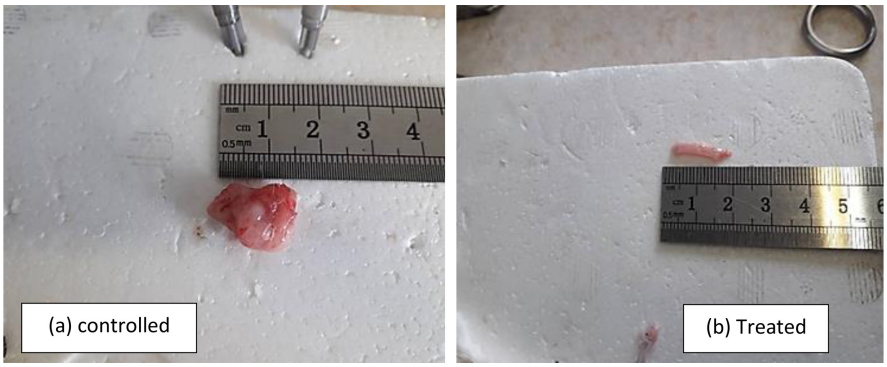

Figure S15. Very interesting results compare the cancerous tumor growing in the breast of the animal from the control group (a) versus the therapeutic effect of the manufactured nanodrug in the group of animals treated orally. This research shows a unique possibility in this new nanomedicine, which currently has no equivalent, to be very useful for treating breast cancer, whereas there is no need for chemotherapy and radiotherapy during the treatment.